Supporting Information for:

A redox-switchable gold(I) complex for the hydroamination of acetylenes: a convenient way for studying ligand-derived electronic effects

César Ruiz-Zambrana, Macarena Poyatos and Eduardo Peris

Institute of Advanced Materials (INAM). Centro de Innovación en Química Avanzada (ORFEO-CINQA). Universitat Jaume I. Av. Vicente Sos Baynat s/n. Castellón. E-12071. Spain. Email: poyatosd@uji.es, eperis@uji.es.

General considerations.

N,N'-Bis-(*n*-butyl)-2,3,6,7-tetra(*n*-butylamino)-1,4,5,8-naphthalenetetracarboxylic diimide (**1**) was prepared according to literature methods.[1] All the other reagents were used as received from the commercial suppliers. Anhydrous solvents were dried using a solvent purification system (SPS M BRAUN) or purchased and degassed prior to use by purging them with dry nitrogen. NMR spectra were recorded on a Bruker 300 MHz, using $CDCl_3$ as solvent. Electrospray mass spectra (ESI-MS) were recorded on a Micromass Quatro LC instrument; nitrogen was employed as drying and nebulizing gas. UV-Visible absorption spectra were recorded on a Varian Cary 300 BIO spectrophotometer using dry and degassed dichloromethane under ambient conditions. Emission spectra were recorded on a modular Horiba FluoroLog-3 spectrofluorometer employing dry and degassed dichloromethane.

1. Synthesis and characterization of compounds

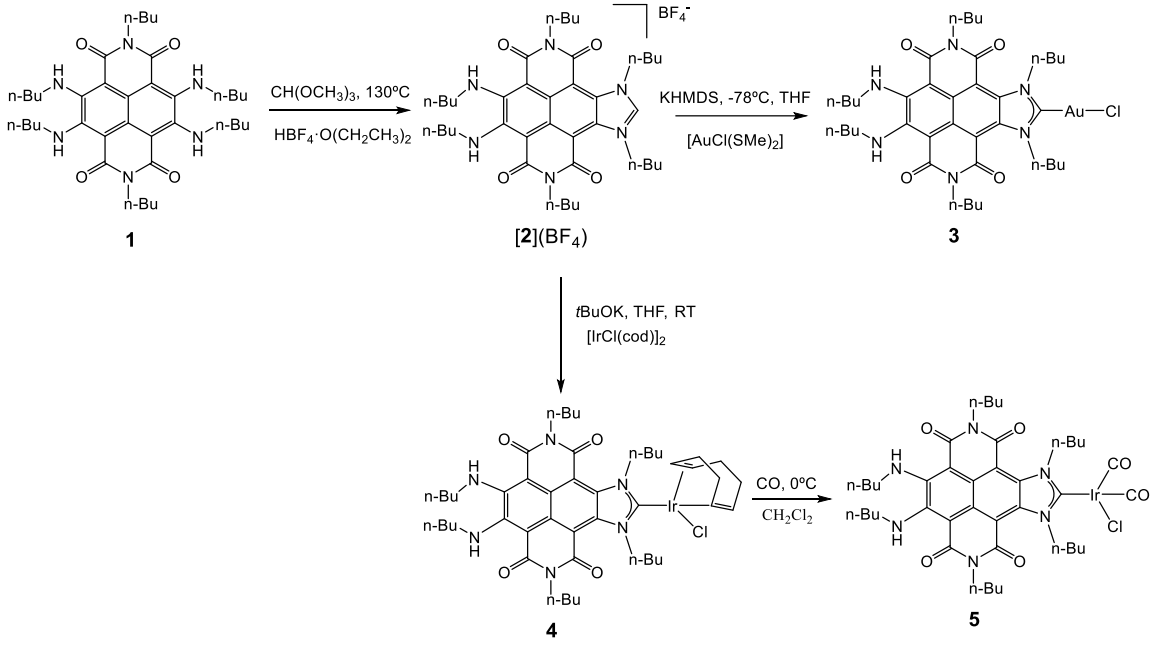

Scheme S1. Synthesis of the NDI-NHC complexes

Synthesis and characterization of imidazolium salt [2](BF$_4$). N,N'-Bis-(n-butyl)-2,3,6,7-tetra(*n*-butylamino)-1,4,5,8-naphthalenetetracarboxylic diimide (500 mg, 0.75 mmol, 1 equiv.), HBF$_4$ (54 % in diethyl ether, 120 µL, 0.9 mmol, 1.2 equiv.) and trimethyl orthoformate (7 mL) were placed together in a Schlenk tube fitted with a Teflon cap. The solution was slowly heated to 130 °C under continuous stirring overnight. After this time, the mixture was allowed to reach room temperature. The Schlenk tube was carefully opened. Diethyl ether was added to the reaction mixture and the precipitated solid was collected by filtration. In order to purify the obtained solid, it was dissolved in the minimum amount of dichloromethane and precipitated again with diethyl ether. The desired compound was isolated by filtration as a reddish crystalline solid in 70% yield (353.5 mg). **^{1}H NMR** (300 MHz, $CDCl_3$): δ 10.95 (t, $^3J_{H\text{-}H}$ = 6 Hz, 2H, RR'N*H*), 9.70 (s, 1H, NC*H*N), 5.09 (t, $^3J_{H\text{-}H}$ = 8 Hz, 4H, CH_2 imid. butyl), 4.23 (t, $^3J_{H\text{-}H}$ = 8 Hz, 4H, CH_2 napht. butyl), 3.71 (q, $^3J_{H\text{-}H}$ = 8 Hz, 4H, CH_2 amine butyl), 1.80-1.53 (m, 12H, CH_2 butyl), 1.53-1.29 (m, 12H, CH_2 butyl), 1.01 (t, $^3J_{H\text{-}H}$ = 8 Hz, 6H, CH_3 butyl), 0.92 (t, $^3J_{H\text{-}H}$ = 8 Hz, 12H, CH_3

$_{butyl}$).**^{13}C{^{1}H} NMR** (75 MHz, $CDCl_3$): δ 165.6 (*C*=O, C_6), 160.8 (*C*=O, C_6), 152.2 (C_1), 147.4 (N*C*HN, C_7), 129.3 (C_5), 125.1 (C_3), 110.9 (C_4), 101.8 (C_2), 54.0 (C_{10}), 47.4 (C_8), 40.9 (C_9), 33.8 (C_{11}), 32.3 (C_{13}), 30.3 (C_{12}), 20.5 (C_{14}), 20.2 (C_{14}), 19.5 (C_{14}), 14.0 (C_{15}), 13.8 (C_{15}), 13.7 (C_{15}). **Electrospray MS** (20 V, *m/z*): 673.736 $[M - (BF_4)]^+$ (Calcd. for $[M - (BF_4)]^+$: 673.907).

Synthesis and characterization of NDI-NHC-Au complex 3. Imidazolium salt [**2**](BF_4) (50 mg, 0.07 mmol, 1 equiv.), KHMDS (0.5M in toluene, 144 µL, 0.072 mmol, 1.1 equiv.) and the metal precursor [AuCl(SMe)$_2$] (19.4 mg, 0.07 mmol, 1 equiv.) were placed together in a Schlenk flask containing pre-activated molecular sieves (4 Å). Dry and previously deoxygenated THF (7 mL) was added at -78ºC. The mixture was allowed to reach room temperature overnight under the exclusion of light. Once at room temperature, a spatula of charcoal was added and the mixture was stirred for further 30 minutes. The mixture was filtered through Celite using CH_2Cl_2. The solvent was then removed under reduced pressure. The crude product was purified by column chromatography using CH_2Cl_2 as eluent. Complex 3 was isolated as a pink solid in 44% yield (26 mg). **^{1}H NMR** (300 MHz, $CDCl_3$): δ 10.54 (t, $^{3}J_{H\text{-}H}$ = 6 Hz, 2H, RR'N*H*), 5.32 (t, $^{3}J_{H\text{-}H}$ = 8 Hz, 4H, C$H_{2\ \text{imid. butyl}}$), 4.23 (t, $^{3}J_{H\text{-}H}$ = 8 Hz, 4H, C$H_{2\ \text{napht. butyl}}$), 3.63 (q, $^{3}J_{H\text{-}H}$ = 8 Hz, 4H, C$H_{2\ \text{amine butyl}}$), 1.80-1.43 (m, 12H, C$H_{2\ \text{butyl}}$), 1.18-1.03 (m, 12H, C$H_{2\ \text{butyl}}$), 1.01 (t, $^{3}J_{H\text{-}H}$ = 8 Hz, 6H, C$H_{3\ \text{butyl}}$), 0.95-0.81 (m, 12H, C$H_{3\ \text{butyl}}$). **^{13}C{^{1}H} NMR** (75 MHz, $CDCl_3$): δ 186.6 (Au-C_7), 166.0 (*C*=O, C_6), 161.2 (*C*=O, C_6), 151.4 (C_1), 131.5 (C_5), 122.6 (C_3), 110.0 (C_4), 103.3 (C_2), 54.3 (C_{10}), 46.8 (C_8), 40.8 (C_9), 33.8 (C_{11}), 31.9 (C_{13}), 29.8 (C_{12}), 20.5 (C_{14}), 20.3 (C_{14}), 19.8 (C_{14}), 14.0 (C_{15}), 13.9 (C_{15}), 13.8 (C_{15}).

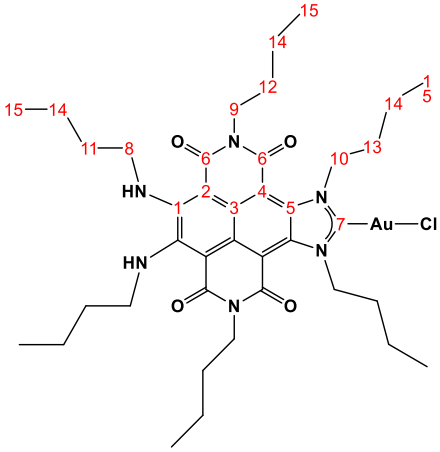

Synthesis and characterization of NDI-NHC-Ir complex 4. [**2**](BF$_4$) (100 mg, 0.13 mmol, 1 equiv.), [IrCl(cod)]$_2$ (43.7 mg, 0.07 mmol, 0.5 equiv.) and tBuOK (32.1 mg, 0.29 mmol, 2.2. equiv.) were placed together in a Schlenk flask containing pre-activated molecular sieves (4 Å). Dry and previously deoxygenated THF (10 mL) was added. The resulting mixture was stirred at room temperature overnight. The mixture was filtered through Celite. The solvent was then removed under reduced pressure. The crude product was purified by column chromatography using CH_2Cl_2 as eluent. After purification, complex 4 was isolated as a purple solid(51.8 mg, 43%). **^{1}H NMR** (300 MHz, $CDCl_3$): δ 10.22 (t, $^3J_{H\text{-}H}$ = 6 Hz, 2H, RR'N*H*), 5.95-5.75 (m, 2H, C*H*$_2$ imid. butyl), 5.37-5.22 (m, 2H, C*H*$_2$ imid. butyl), 4.87-4.72 (m, 2H, C*H*$_{cod}$), 4.39-4.06 (m, 4H, C*H*$_2$ napht. butyl), 3.58 (q, $^3J_{H\text{-}H}$ = 9 Hz, 4H, C*H*$_2$ amine butyl), 3.22-3.08 (m, 4H, C*H*$_{cod}$), 2.44-2.20 (m, 4H, C*H*$_2$ cod), 1.95-1.64 (m, 4H, C*H*$_2$ cod), 1.54-1.18 (m, 24H, C*H*$_2$ butyl), 1.01 (t, $^3J_{H\text{-}H}$ = 6 Hz, 6H, C*H*$_3$ butyl), 0.97-0.86 (m, 12H, C*H*$_3$ butyl). **^{13}C{^{1}H} NMR** (75 MHz, $CDCl_3$): δ 200.8 (Ir-*C*$_7$), 166.3 (*C*=O, *C*$_6$), 161.5 (*C*=O, *C*$_6$), 151.0 (*C*$_1$), 134.0 (*C*$_5$), 120.4 (*C*$_3$), 108.6 (*C*$_4$), 104.6 (*C*$_2$), 86.6 (*C*$_{cod}$), 53.7 (*C*$_{cod}$), 53.0 (*C*$_{10}$), 46.4 (*C*$_8$), 40.7 (*C*$_9$), 33.8 (*C*$_{11}$), 33.7 (*C*$_{cod}$) 30.4 (*C*$_{13}$), 29.8 (*C*$_{12}$), 29.7 (*C*$_{cod}$), 20.6 (*C*$_{14}$), 20.3 (*C*$_{14}$), 20.0 (*C*$_{14}$), 14.0 (*C*$_{15}$), 13.9 (*C*$_{15}$), 13.9 (*C*$_{15}$).

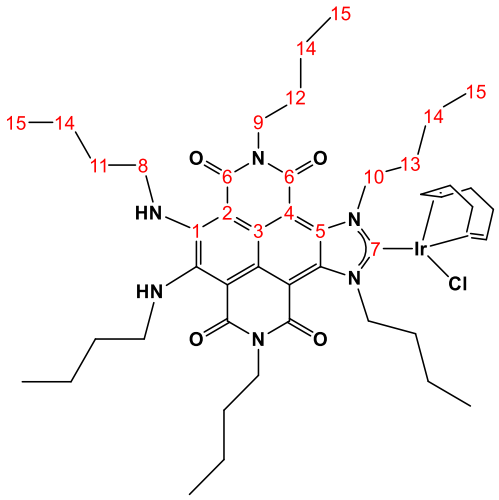

Synthesis and characterization of NDI-NHC-Ir-CO complex 5. CO gas (1 atm, 10 mL/min) was passed through a solution of complex **4** (20 mg, 0.02 mmol) in dichloromethane (10 mL) for 45 minutes at 0 ºC. An immediate colour change from purple to pink was observed. The solvent was removed under reduced pressure, giving the desired carbonyl derivative (**5**) (15.2 mg, 73%).**^{1}H NMR** (300 MHz, $CDCl_3$): δ 10.49 (t, $^3J_{H\text{-}H}$ = 6 Hz, 2H, RR'N*H*), 5.56-5.23 (m, 4H, C*H*$_2$ imid. butyl), 4.37-4.13 (m, 4H, C*H*$_2$ napht. butyl), 3.63 (q, $^3J_{H\text{-}H}$ = 6 Hz, 4H, C*H*$_2$ amine butyl), 1.86-1.33 (m, 24H, C*H*$_2$ butyl), 1.01 (t, $^3J_{H\text{-}H}$ = 6 Hz, 6H, C*H*$_3$ butyl), 0.96-0.84 (m, 12H, C*H*$_3$ butyl). **^{13}C{^{1}H}** NMR (75 MHz,

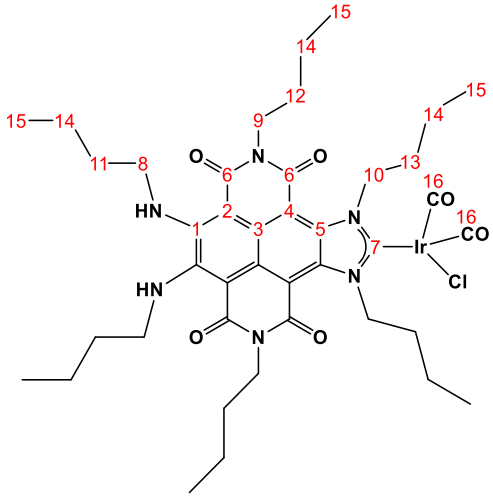

$CDCl_3$): δ 189.3 (Ir-C_7), 180.9 (C=O, C_{16}), 168.1 (C=O, C_{16}), 166.1 (C=O, C_6), 161.2 (C=O, C_6), 151.4 (C_1), 132.5 (C_5), 122.1 (C_3), 110.0 (C_4), 103.5 (C_2), 54.1 (C_{10}), 46.7 (C_8), 40.8 (C_9), 33.8 (C_{11}), 31.1 (C_{13}), 30.4 (C_{12}), 20.6 (C_{14}), 20.3 (C_{14}), 19.9 (C_{14}), 14.0 (C_{15}), 13.9 (C_{15}), 13.8 (C_{15}). **IR** (CH_2Cl_2): 1987.3 (ν Ir-CO) and 2068.3 (ν Ir-CO) cm^{-1}.

2. Spectroscopic data

2.1. ^{1}H, ^{13}C, HSQC and HMBC spectra of [2](BF$_4$) in CDCl$_3$

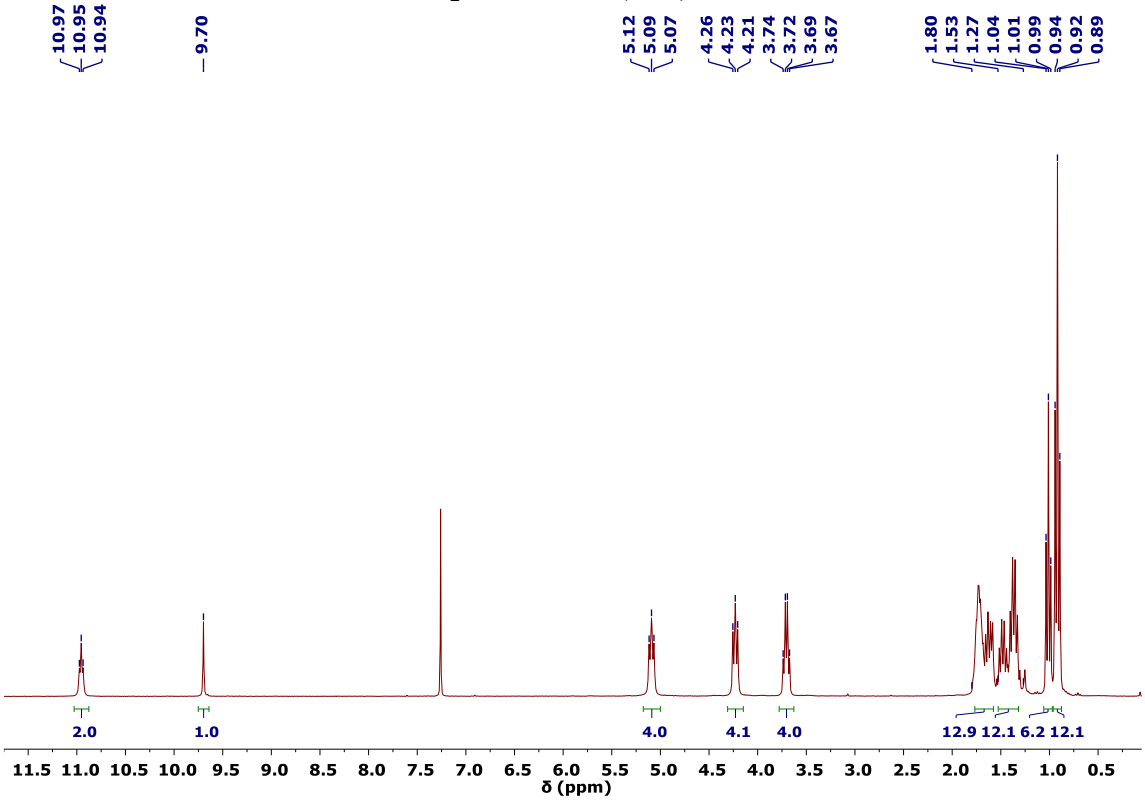

Figure S1. ^{1}H NMR spectrum (300 MHz, CDCl$_3$) of [**2**](BF$_4$)

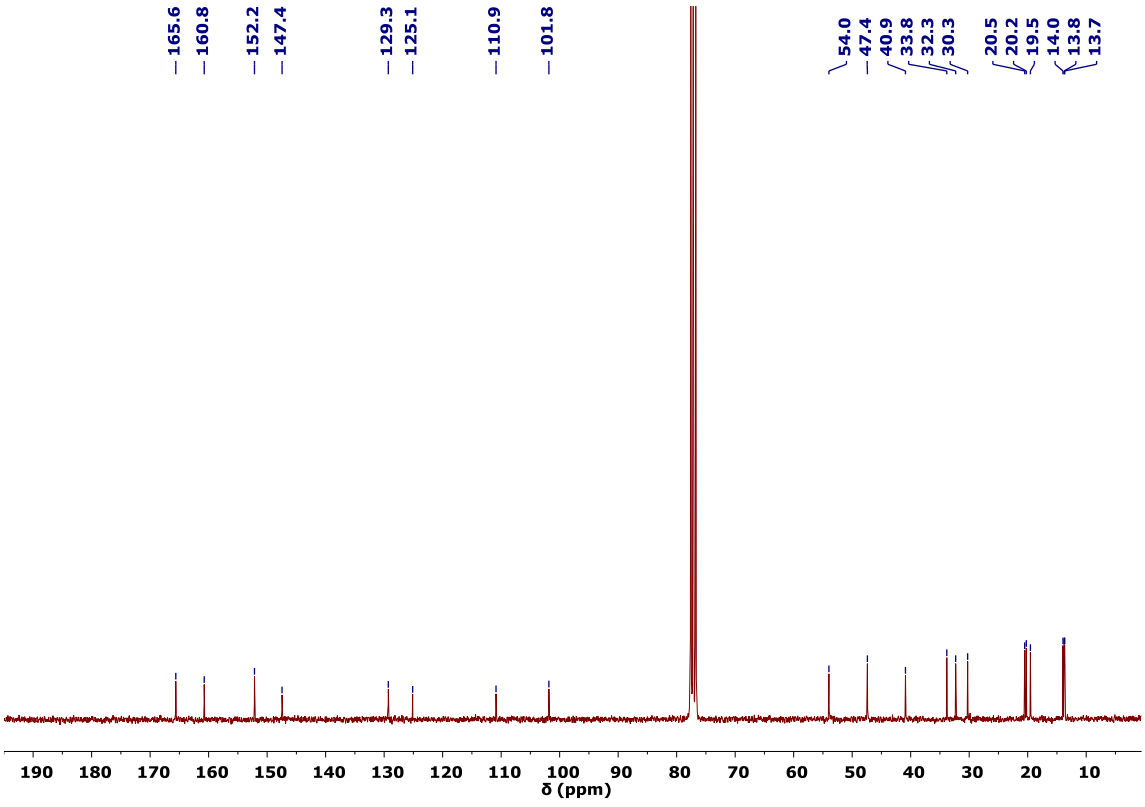

Figure S2. $^{13}C\{^{1}H\}$ spectrum (75 MHz, CDCl$_3$) of [**2**](BF$_4$)

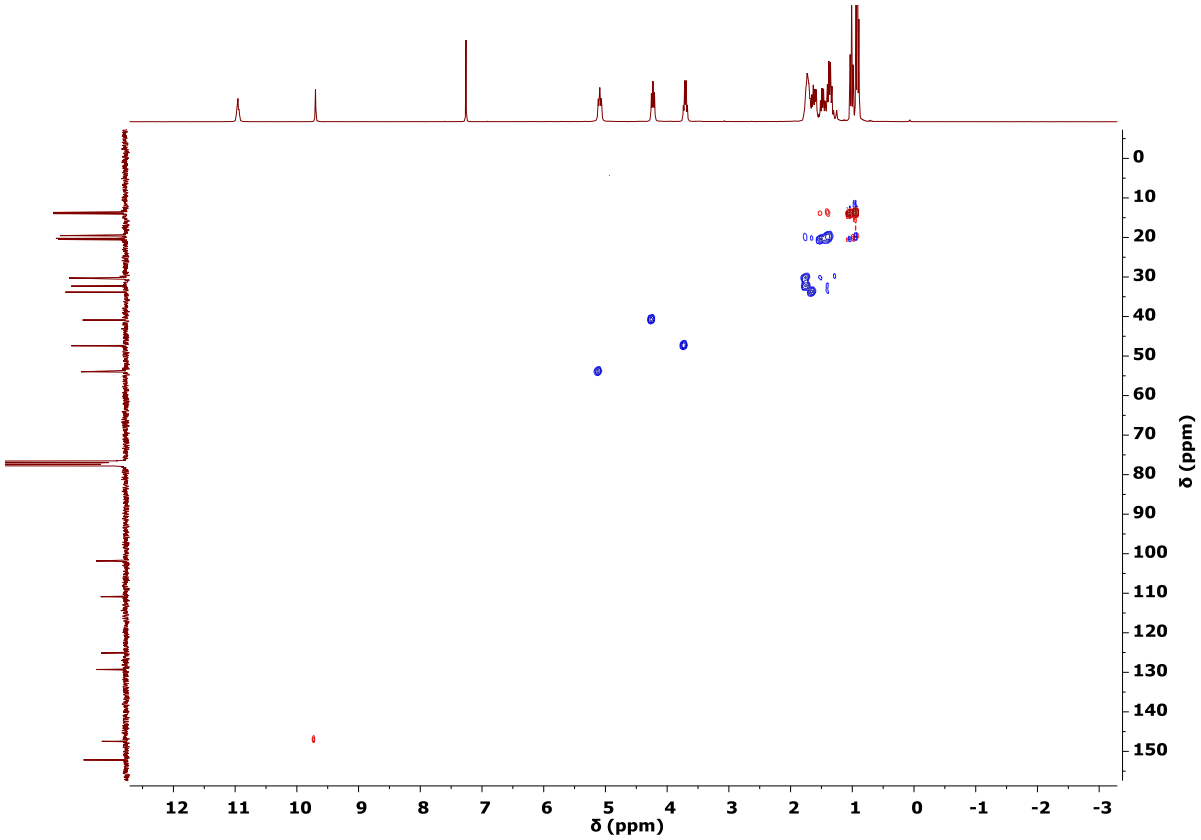

Figure S3. ^{1}H-^{13}C HSQC spectrum (300 MHz, $CDCl_3$) of [**2**](BF_4)

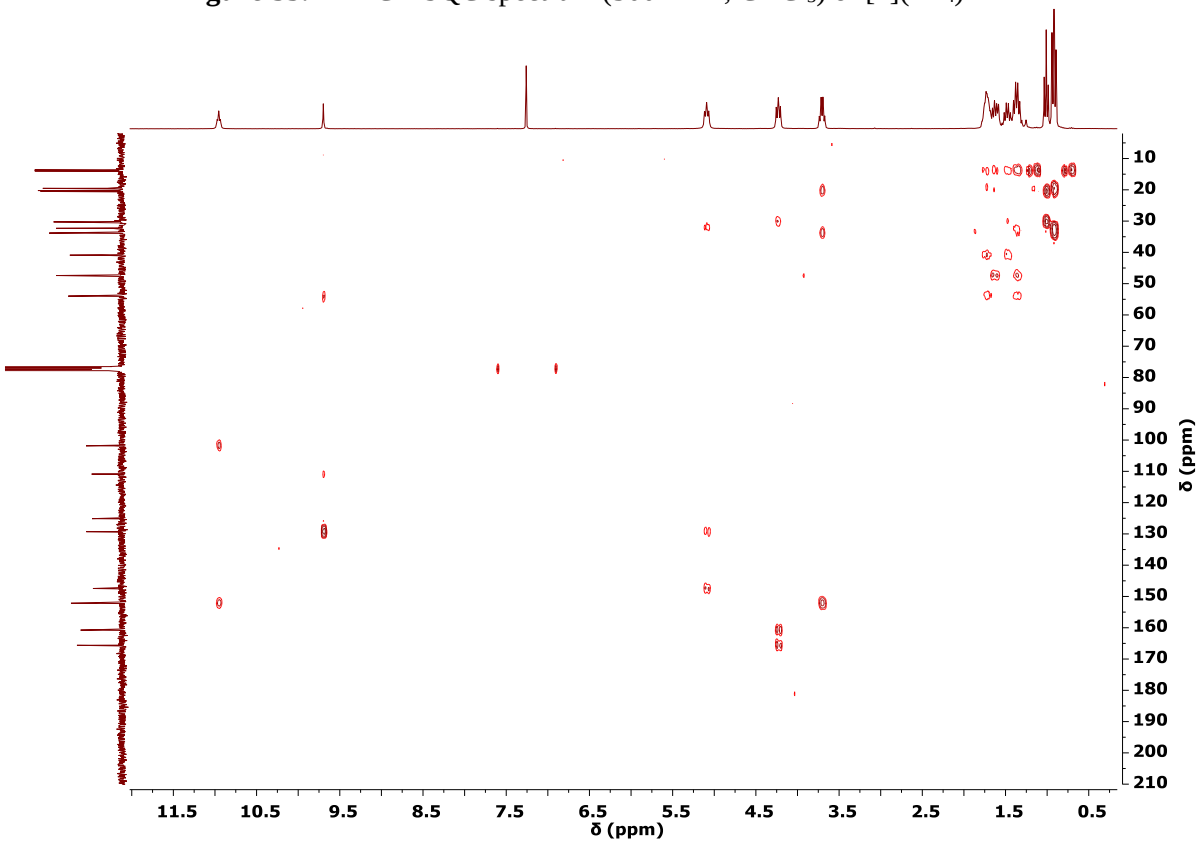

Figure S4. ^{1}H-^{13}C HMBC spectrum (300 MHz, $CDCl_3$) of [**2**](BF_4)

2.2. ^{1}H, ^{13}C, HSQC and HMBC spectra of 3 in $CDCl_3$

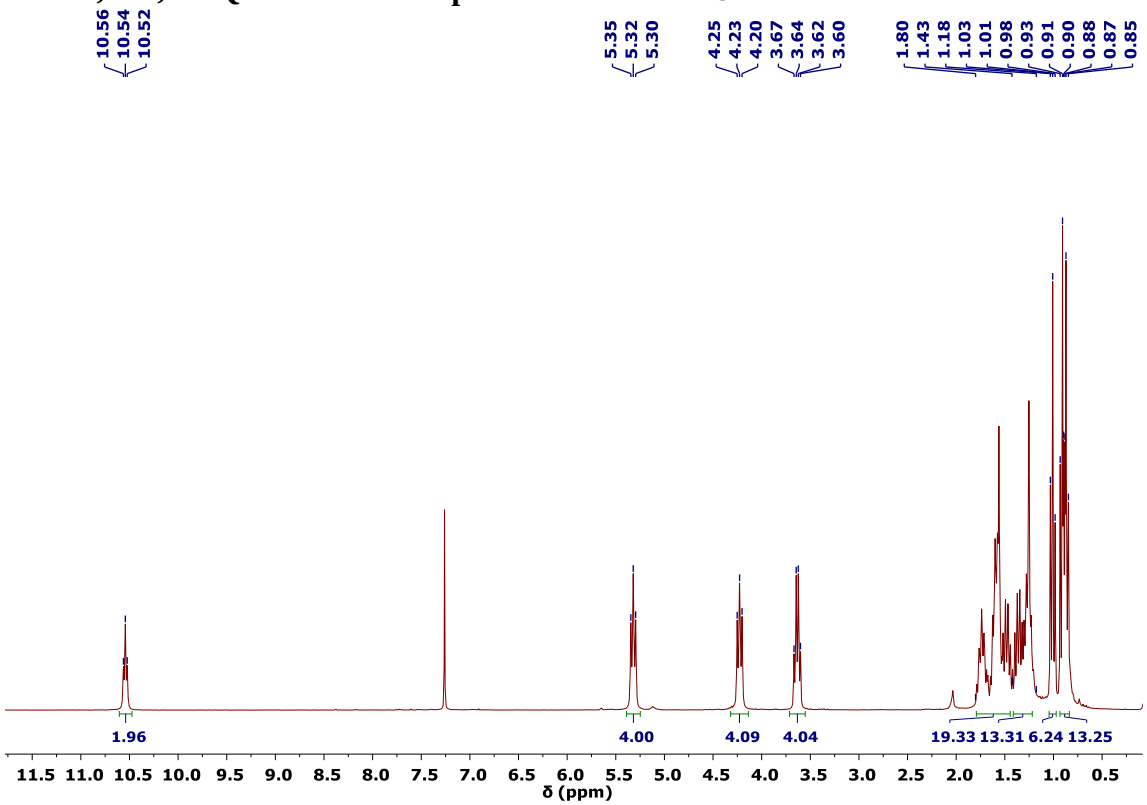

Figure S5. ^{1}H NMR spectrum (300 MHz, $CDCl_3$) of **3**

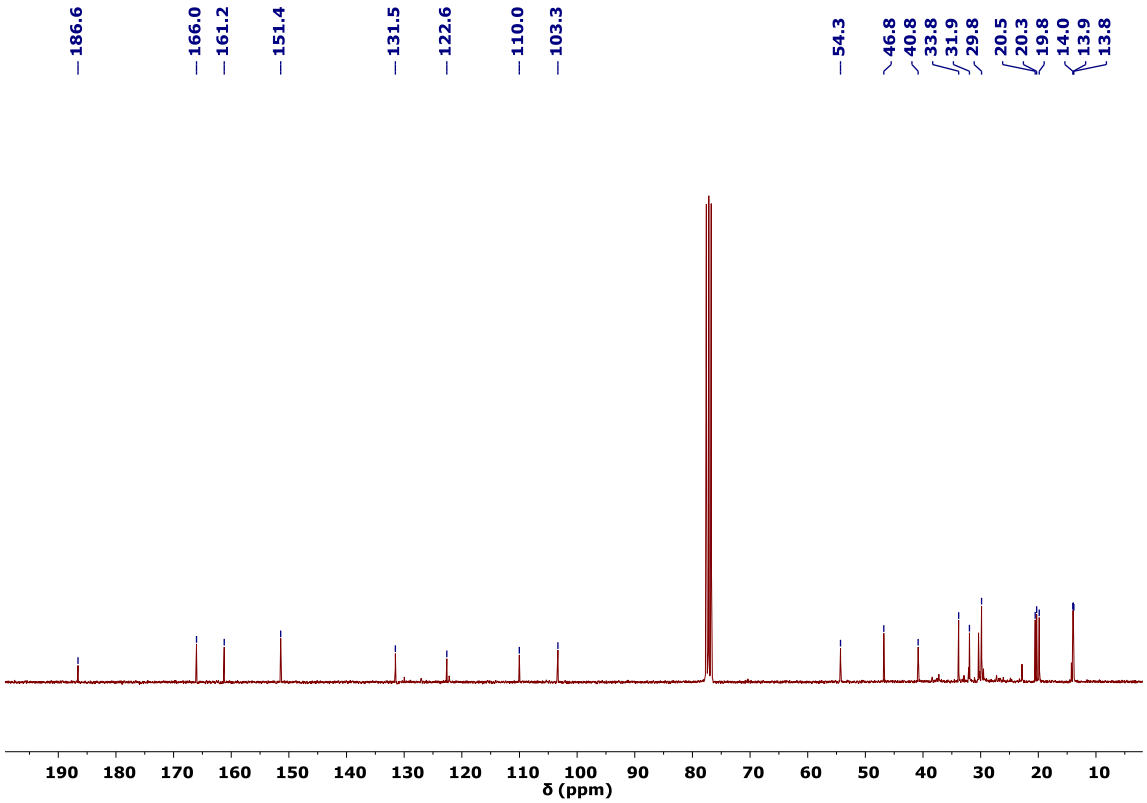

Figure S6. $^{13}C\{^{1}H\}$ spectrum (75 MHz, $CDCl_3$) of **3**

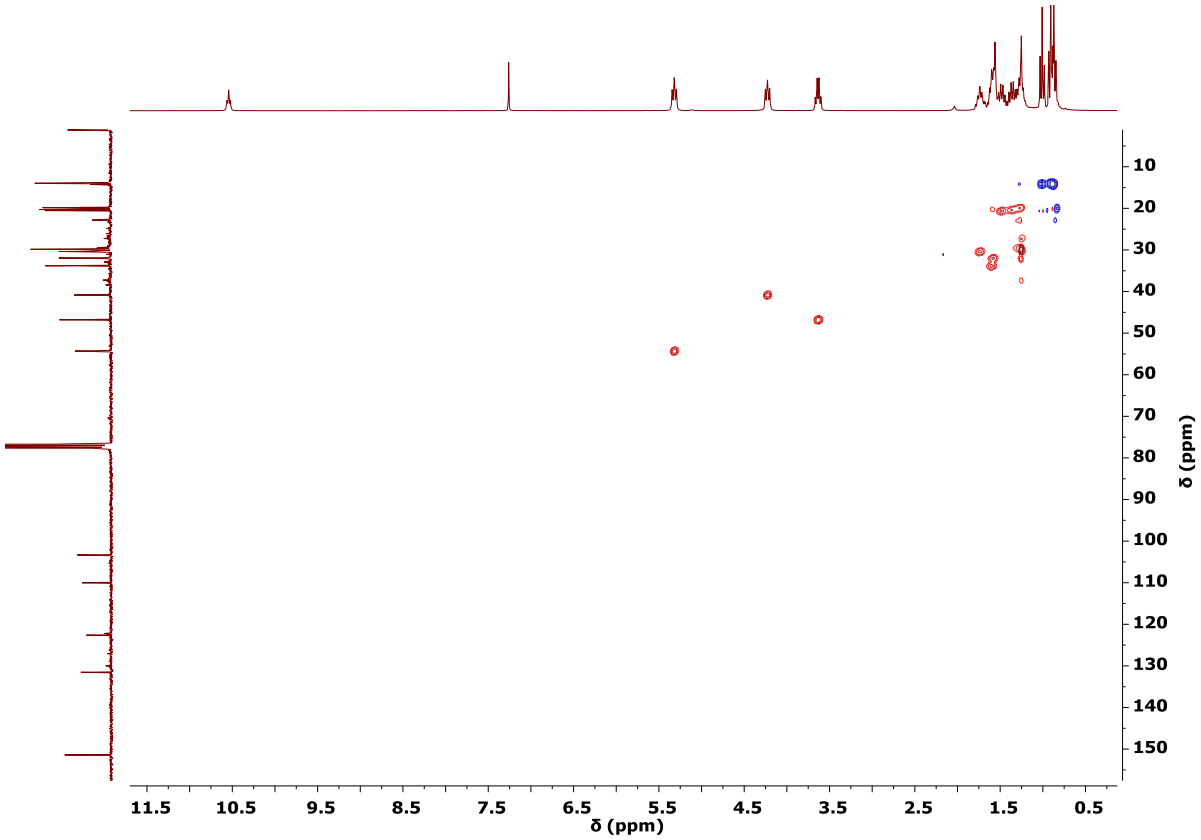

Figure S7. ^{1}H-^{13}C HSQC spectrum (300 MHz, $CDCl_3$) of **3**

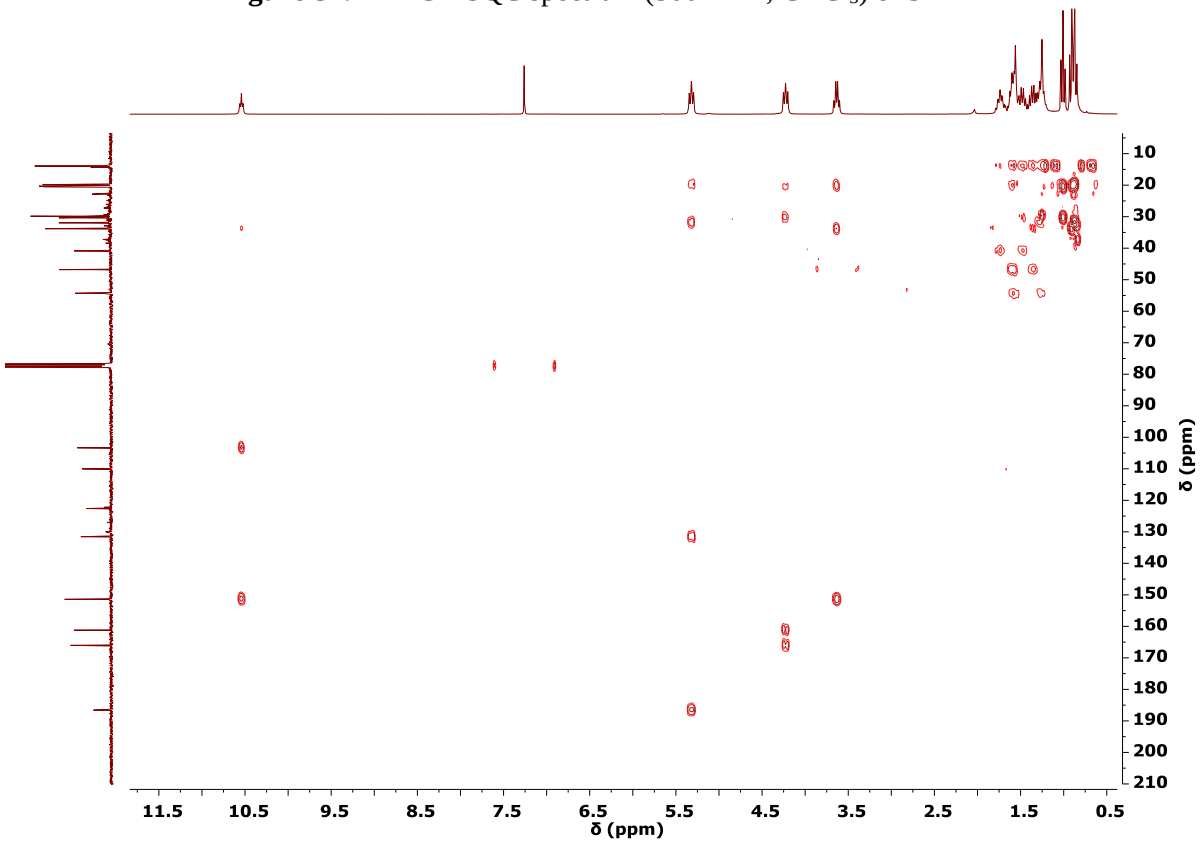

Figure S8. ^{1}H-^{13}C HMBC spectrum (300 MHz, $CDCl_3$) of **3**

2.3. ^{1}H, ^{13}C, HSQC and HMBC spectra of 4 in $CDCl_3$

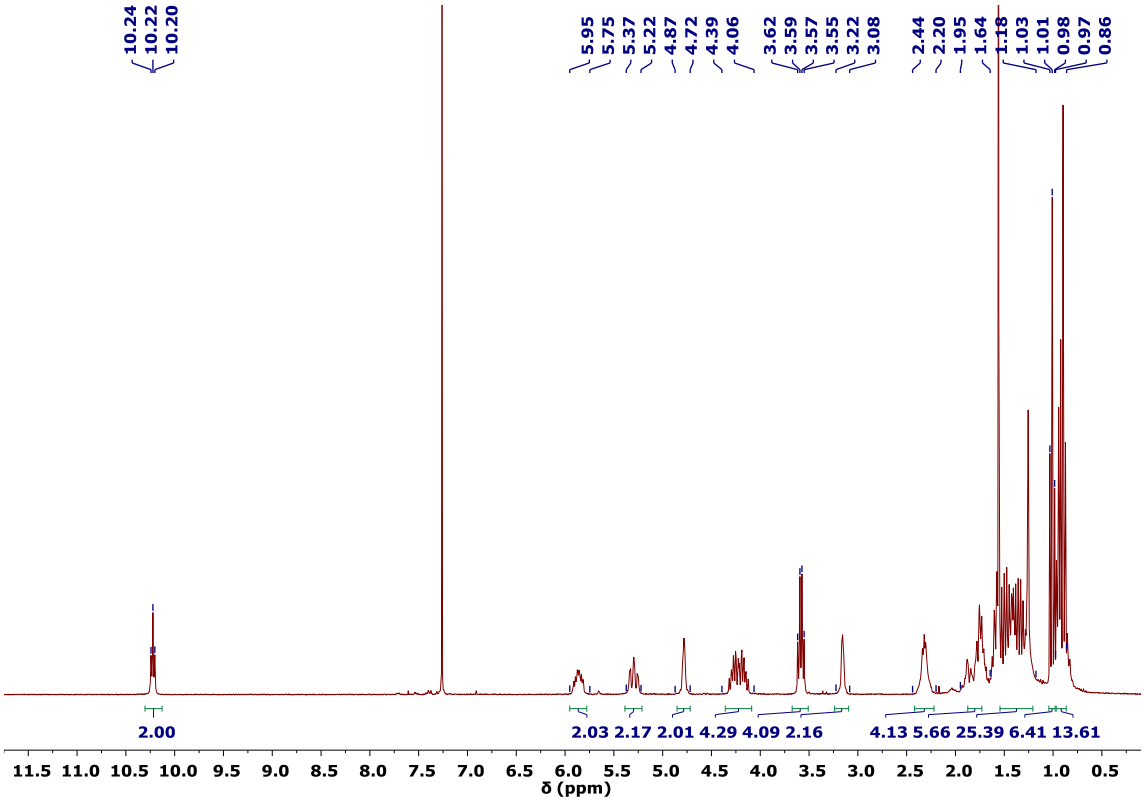

Figure S9. ^{1}H NMR spectrum (300 MHz, $CDCl_3$) of **4**

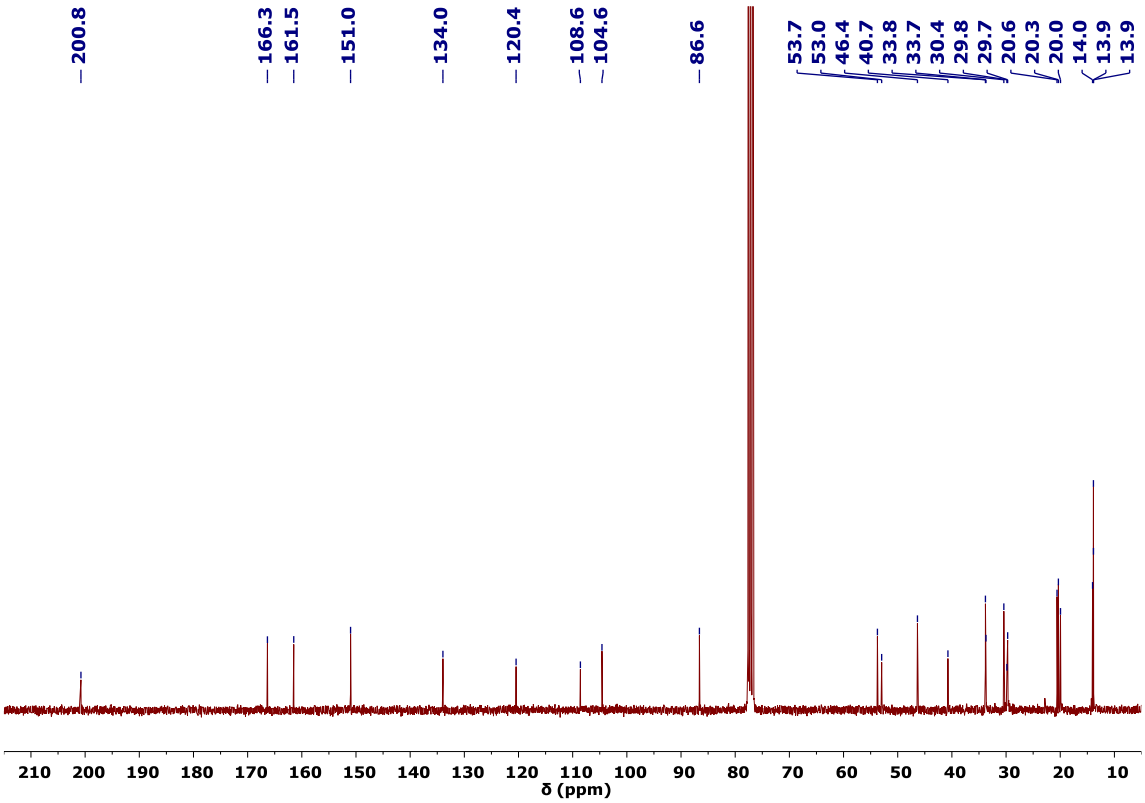

Figure S10. $^{13}C\{^{1}H\}$ spectrum (75 MHz, $CDCl_3$) of **4**

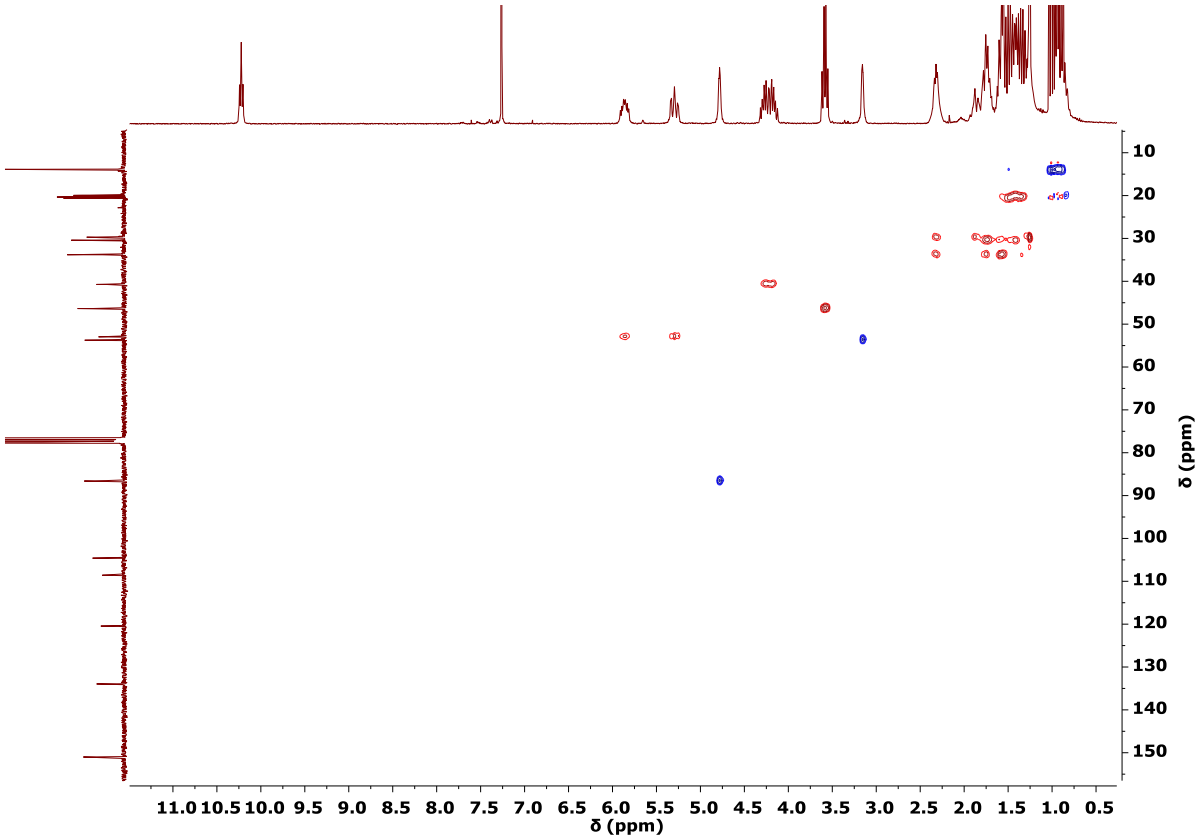

Figure S11. ^{1}H-^{13}C HSQC spectrum (300 MHz, $CDCl_3$) of **4**

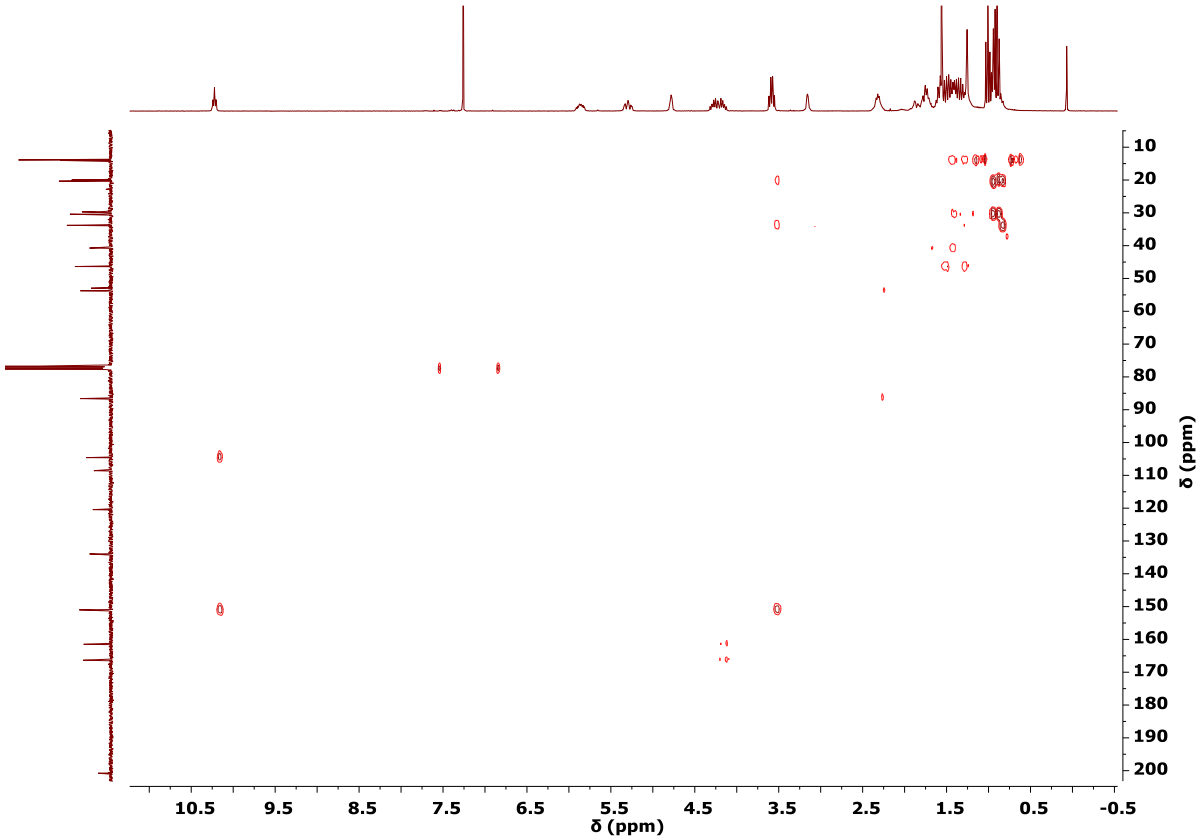

Figure S12. ^{1}H-^{13}C HMBC spectrum (300 MHz, $CDCl_3$) of **4**

2.4. ^{1}H, ^{13}C, HSQC and HMBC spectra of 5 in $CDCl_3$

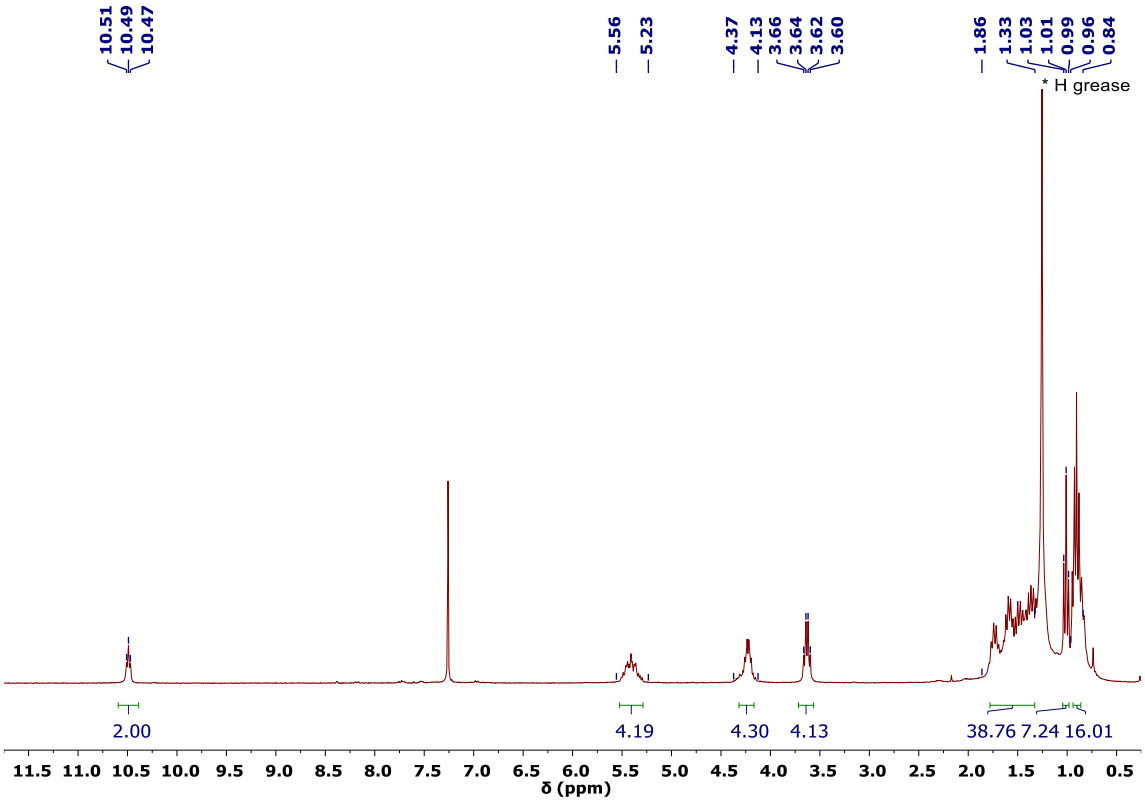

Figure S13. ^{1}H NMR spectrum (300 MHz, $CDCl_3$) of **5**

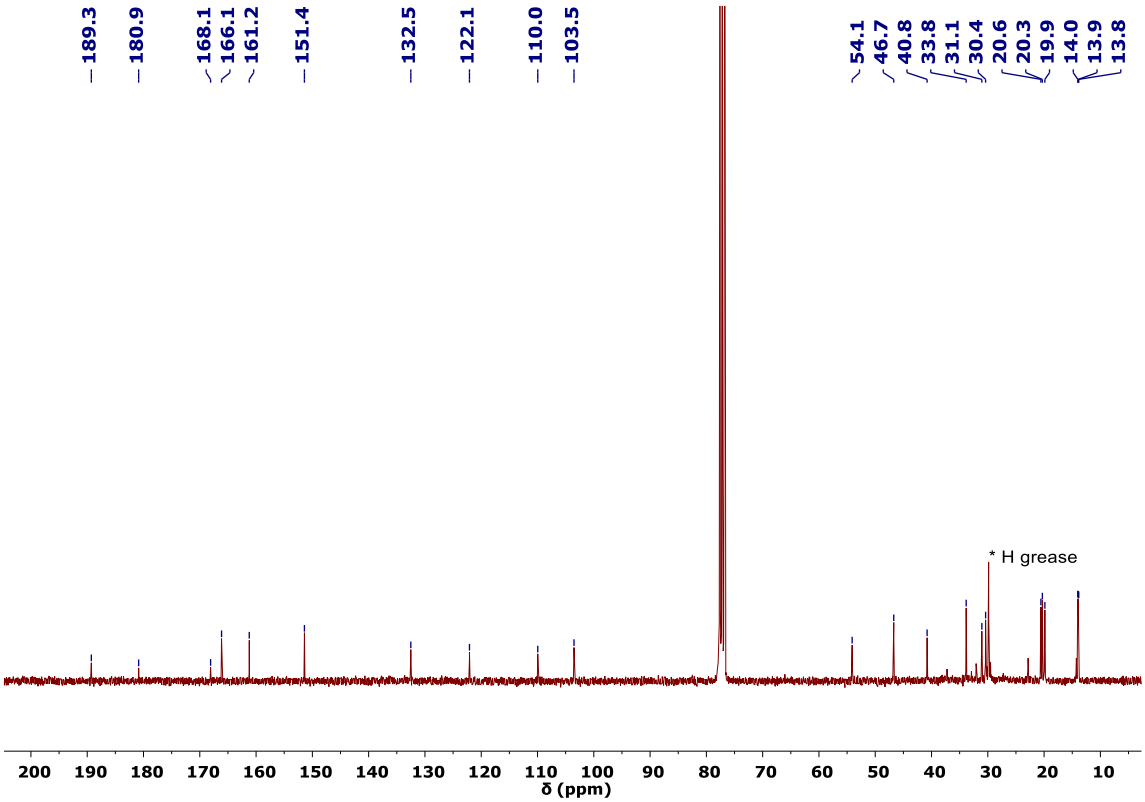

Figure S14. $^{13}C\{^{1}H\}$ spectrum (75 MHz, $CDCl_3$) of **5**

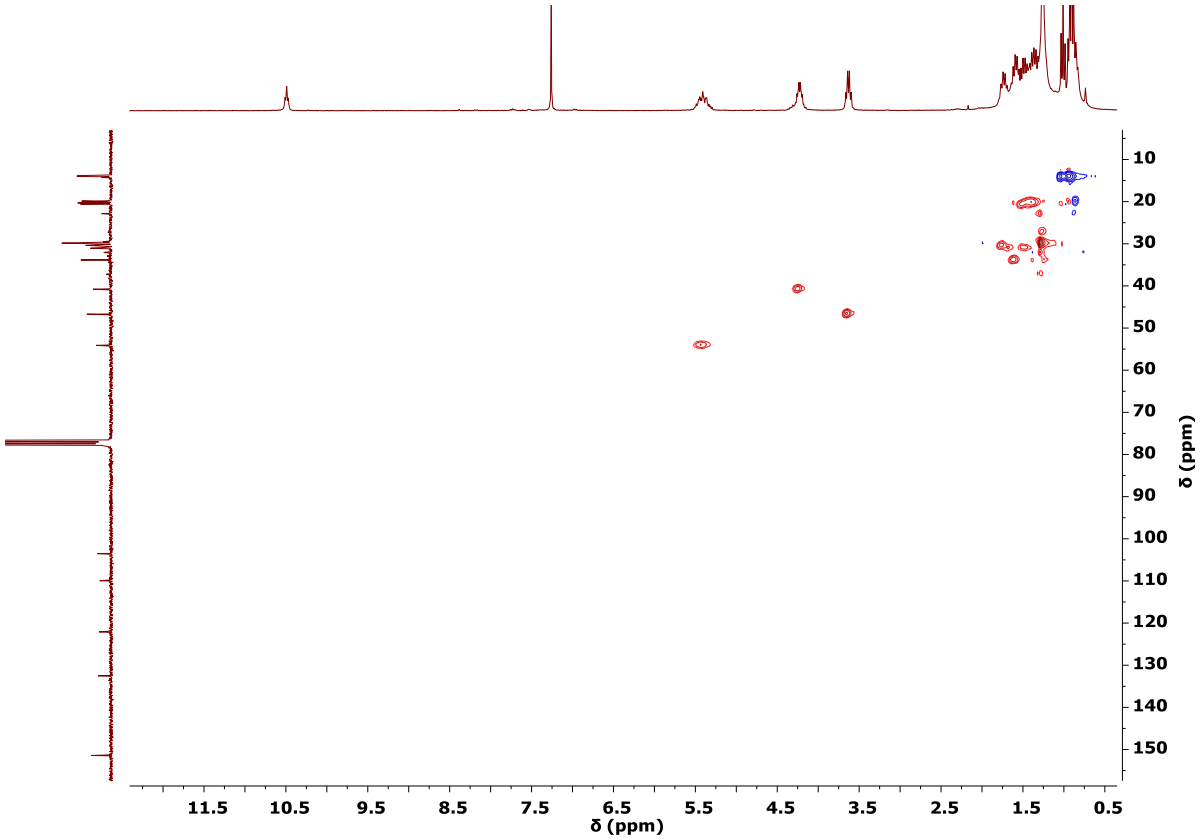

Figure S15. ^{1}H-^{13}C HSQC spectrum (300 MHz, $CDCl_3$) of **5**

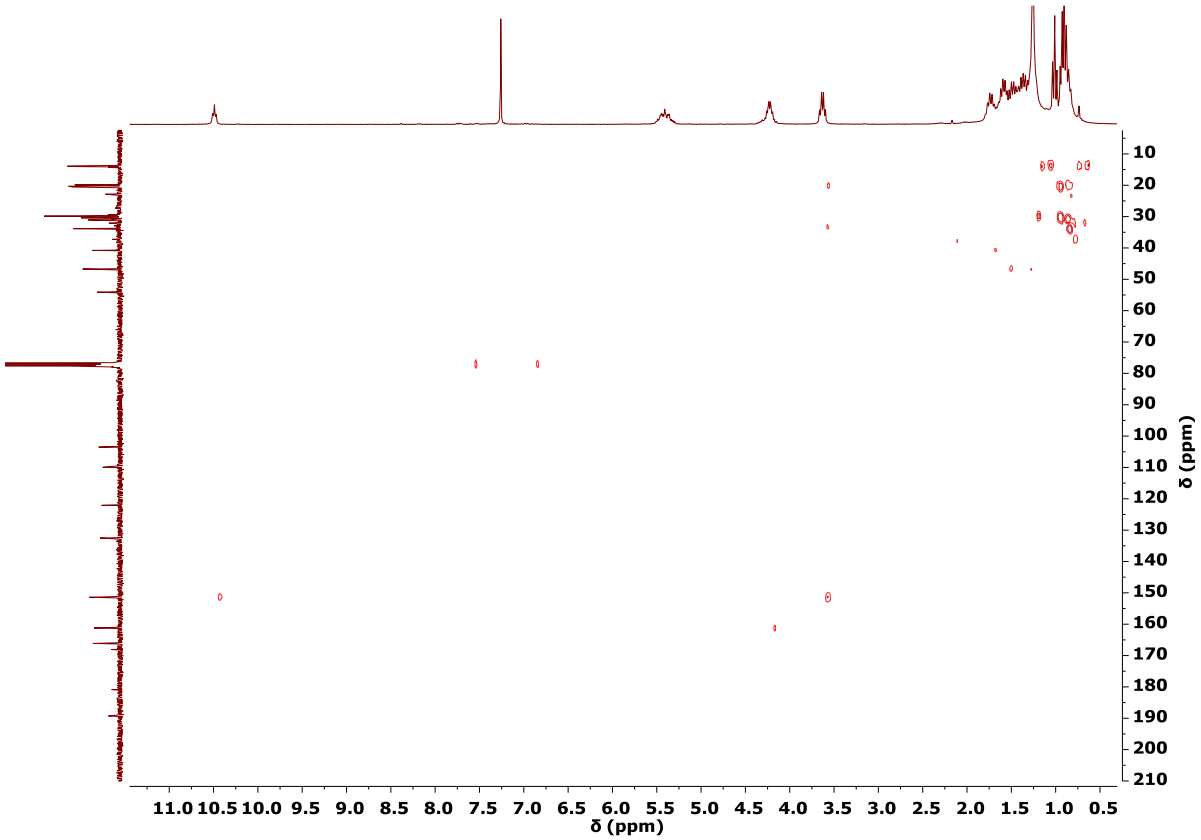

Figure S16. ^{1}H-^{13}C HMBC spectrum (300 MHz, $CDCl_3$) of **5**

3. Electrochemical studies

3.1 Electrochemical measurements

Electrochemical studies were carried out by using an Autolab Potentiostat, Model PGSTAT101 controlled with NOVA 2.1.4 software. In all experiments, $[N(n\text{Bu})_4][PF_6]$ (0.25 M in dry and deoxygenated CH_2Cl_2) was used as the supporting electrolyte with an analyte concentration of 1 mM. Cyclic voltammetry was performed in a cell, under N_2 atmosphere and with disk glassy carbon working electrode, platinum counter electrode, and a silver wire pseudoreference electrode. Measurements were performed at different scan rates. All scans were referenced to the ferrocenium/ferrocene (Fc^+/Fc) couple at 0 V. Ohmic drop was minimized by minimizing the distance between the working and reference electrodes. The residual ohmic drop was estimated by positive feedback and compensated at 95%.

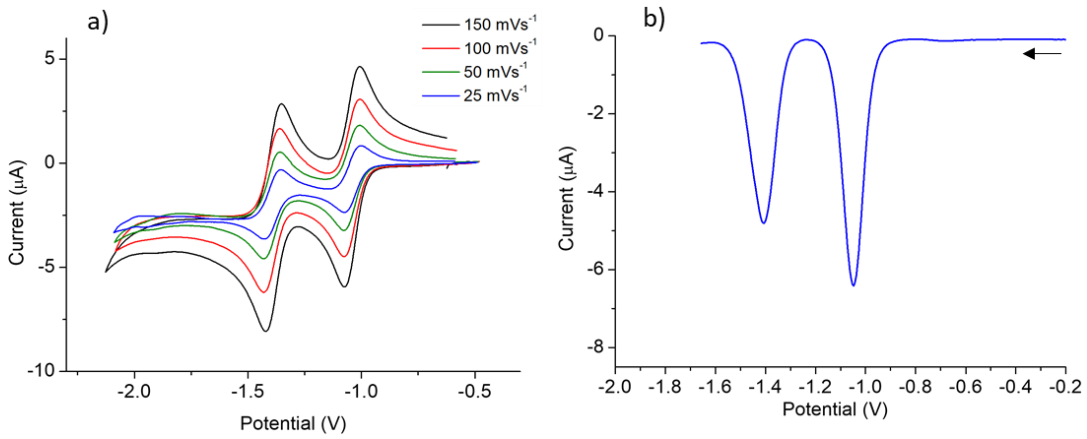

Figure S17. a) Cyclic voltammograms at different scan rates and b) differential pulse voltammetry (50 mV pulse amplitude) of [**2**](BF_4)

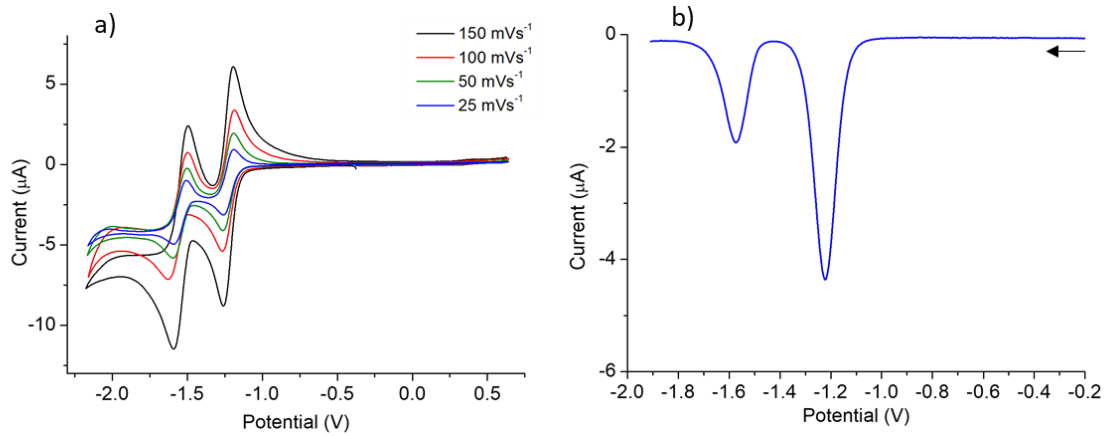

Figure S18. a) Cyclic voltammograms at different scan rates and b) differential pulse voltammetry (50 mV pulse amplitude) of **3**

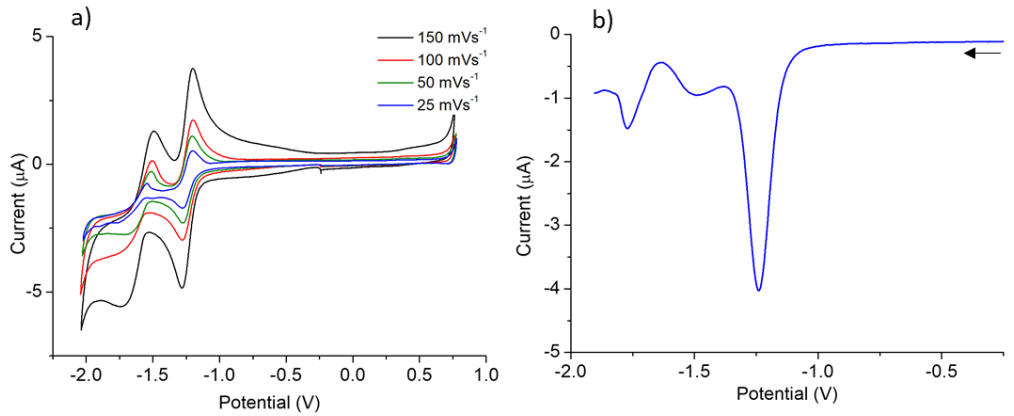

Figure S19. a) Cyclic voltammograms at different scan rates and b) differential pulse voltammetry (50 mV pulse amplitude) of **3** with 2 equiv. of $NaBAR^F$

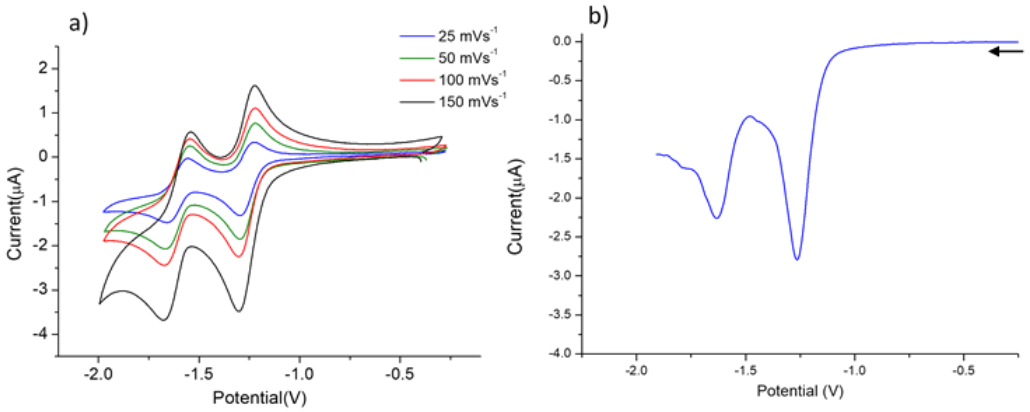

Figure S20. a) Cyclic voltammograms at different scan rates and b) differential pulse voltammetry (50 mV pulse amplitude) of **5**

Table S1. Electrochemical properties of compounds [**2**](BF_4), **3** , **3** + $NaBAR^F$ and **5**

Compounds	$E_{1/2}$ (V)/ΔE (mV)	$E'_{1/2}$ (V)/ΔE (mV)
[**2**](BF_4)	-1.05/53	-1.40/58
3	-1.22/53	-1.55/87[a]
3 + $NaBAR^F$	-1.22/73	-1.49[b]
5	-1.26/65	-1.60/107

[a]The second reduction event is quasi-reversible in **3**. [b]The second reduction event is irreversible in **3** + $NaBAR^F$. The values indicated in the table in both cases correspond to the cathodic peak potential (E_{pc}).

3.2 Spectroelectrochemical measurements

Spectroelectrochemical (SEC) measurements were performed using a gastight, optically transparent thin-layer solution cell fabricated by Prof. Hartl at the University of Reading (Reading, U.K.), as described previously.[2] The SEC cell contained a masked Au-minigrid working electrode (32 wires/cm), a Pt-gauze auxiliary electrode, and an Ag-wire pseudo-reference electrode and had CaF_2 windows. In each experiment, electrochemical reduction of the species of interest ([Analyte] = 0.75 mM for UV-Vis experiments and 3 mM for IR experiments, $[N(n\text{Bu})_4][PF_6]$ = 0.1 M in CH_2Cl_2 under inert atmosphere) was monitored by the appropriate spectroscopy for a period of 2−5 min. First, the potential of the cell was swept negatively starting at the open circuit potential, recording a thin-layer cyclic voltammogram (5 mV/s) to identify the potential window of interest. Then, fresh analyte solution was introduced in the cell and the potential was varied within range of interest in 33 mV steps. The electrolysis step did not exceed 30 s. After each step, an UV-vis spectrum was collected. Diffusion and mixing of the redox products generated at the working and auxiliary electrodes in the cell were reasonably suppressed within the total experimental time (no more than 5 min for one complete measurement). Finally, in order to check the complete reversibility of the processes, a positive potential was applied to the reduced compound to recover the initial species (Figures S21 and S22, green line).

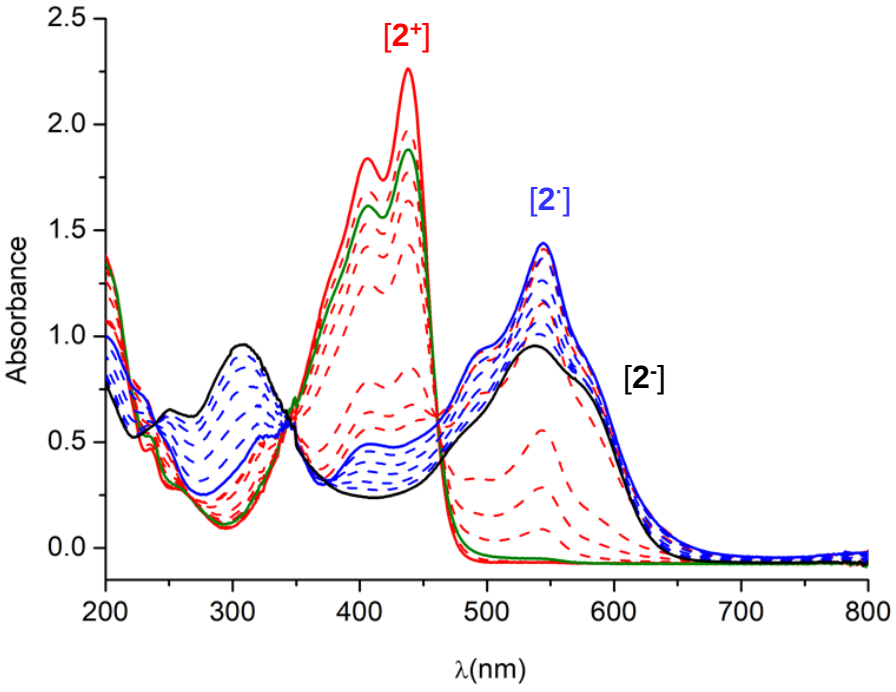

Figure S21. UV-vis SEC monitoring reduction of [**2**](BF_4) in CH_2Cl_2 (0.1 M $[N(nBu)_4][PF_6]$). The solid lines represent the spectra of the starting (red), singly-reduced (blue) and doubly-reduced (black) species. The green line shows the initial compound after applying an oxidation potential to the reduced species.

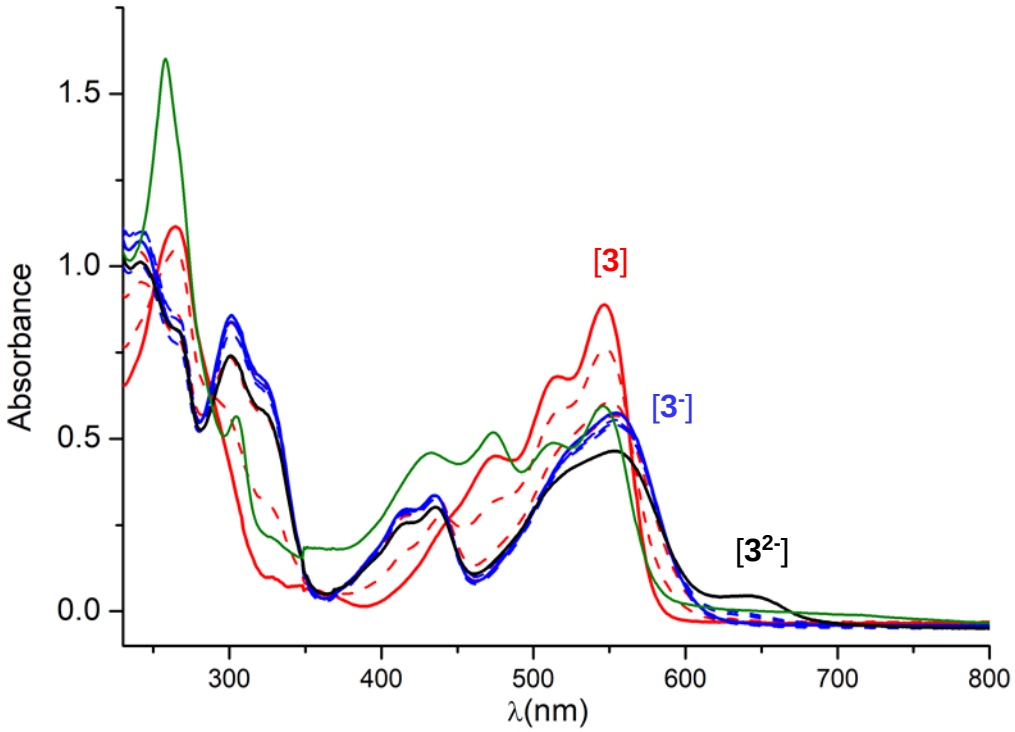

Figure S22. UV-vis SEC monitoring reduction of **3** in CH_2Cl_2 (0.1 M $[N(nBu)_4][PF_6]$). The solid lines represent the spectra of the starting (red), singly-reduced (blue) species. The green line shows the species generated after applying an oxidation potential to the reduced species.

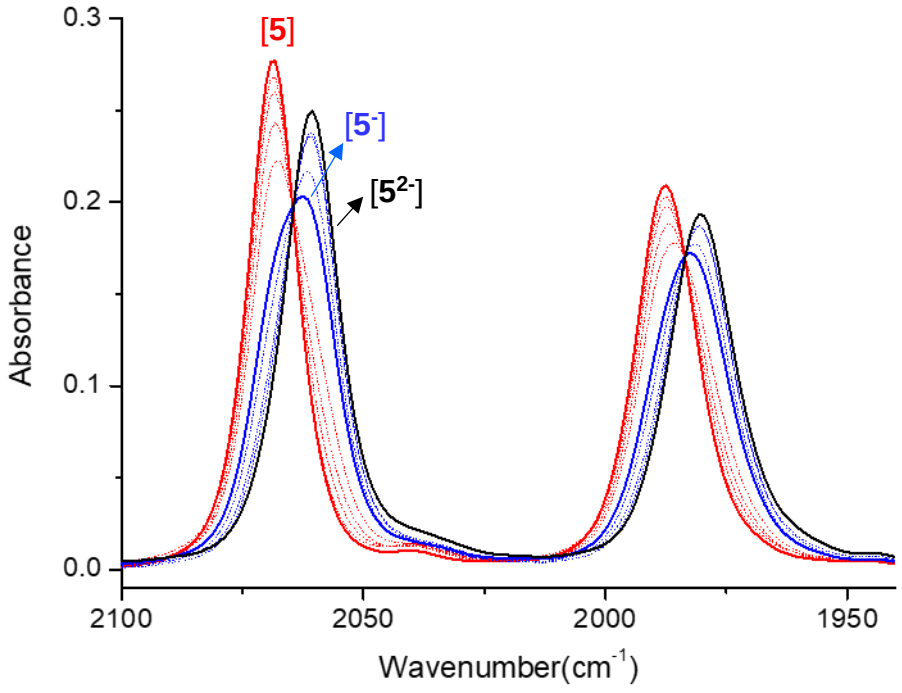

Figure S23. IR-SEC monitoring reduction of **5** in CH_2Cl_2 (0.1 M $[N(nBu)_4][PF_6]$). The solid lines represent the IR spectra of **5** (red), [**5**$^-$] (blue) and [**5**$^{2-}$] (black) species.

4. Photophysical analysis

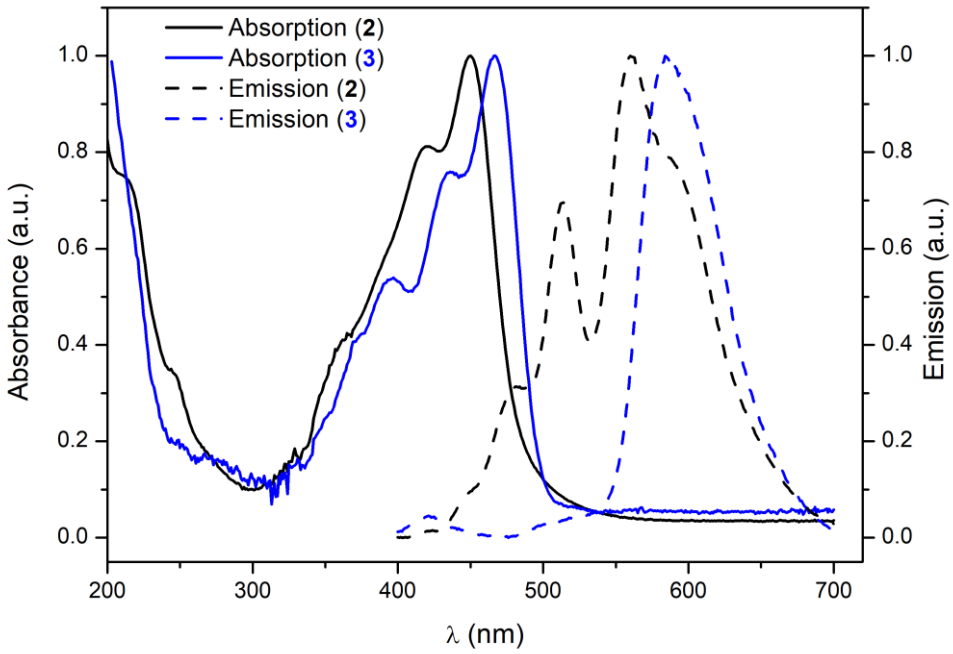

Figure S24. UV-Vis spectra (solid lines) and emission spectra (dashed lines) excited at 375 nm of [**2**](BF_4) (black) and **3** (blue) recorded in CH_2Cl_2 at a concentration of 50 µM.

5. Catalytic studies

5.1 Hydroamination of Phenylacetylene with Aryl Amines

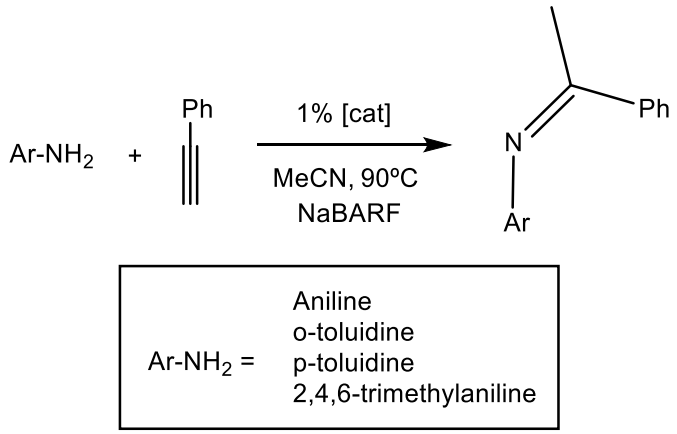

Scheme S2. Hydroamination of phenylacetylene with aryl amines

General procedure. Complex **3** (1 mol %, 0.005 mmol) and $NaBAR^F$ (2 mol %, 0.01 mmol) were placed together in a thick-walled Schlenk tube fitted with a Teflon cap. The mixture was deaerated using vacuum and filled with nitrogen three times. Then, 1 mL of CD_3CN was added, and the reaction mixture was stirred at room temperature for 10 min to activate the catalyst. After this time, the corresponding arylamine (0.55 mmol, 1.1 equiv.), phenylacetylene (0.5 mmol, 1 equiv.), and anisole as internal reference (0.5 mmol, 1 equiv.) were subsequently added under nitrogen. The resulting mixture was stirred at 90°C for the appropriate time. The evolution of the reactions, yields, and conversions were determined by GC analysis. The products were identified by comparison to previously reported data.[3] The time-dependent reaction profile is plotted in the Figure S14. In addition, Table S2 shows the rate constant calculated by plotting the -ln [phenylacetylene] vs. time (Figure S15) assuming first order reaction.

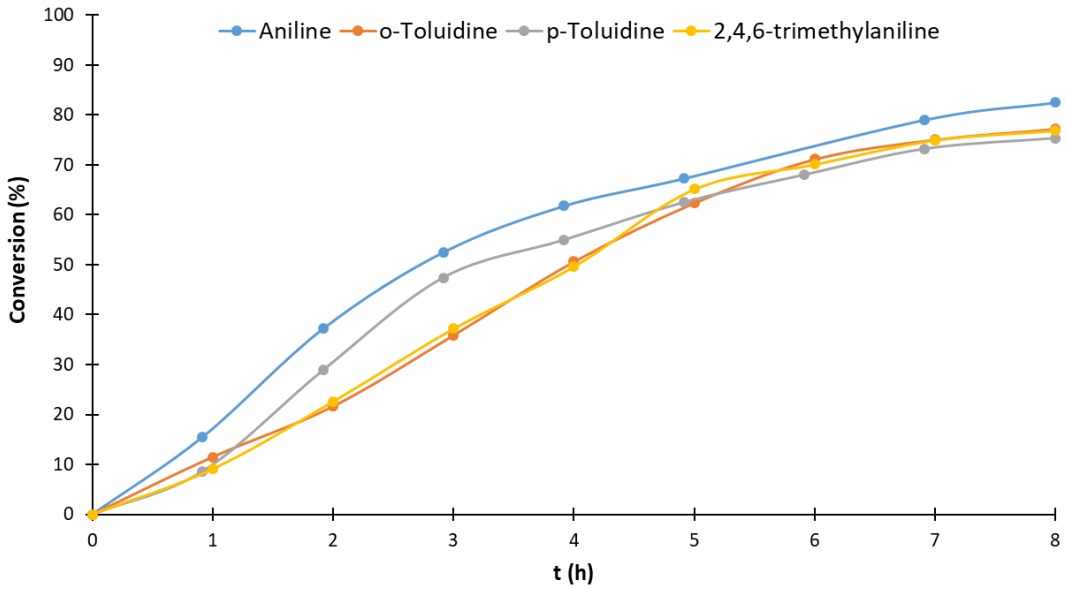

Figure S25. Time-dependent reaction profile of the hydroamination of phenylacetylene with different arylanilines.

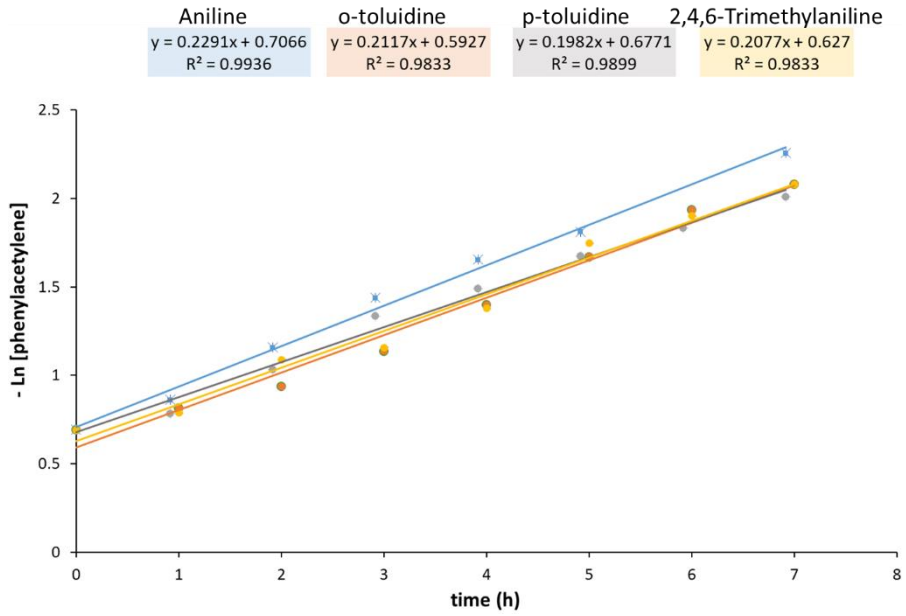

Figure S26. Non-linear least squares fit of the kinetic data assuming first order reaction.

Table S2. Rate constants assuming a reaction order of one.

Entry	Aryl	Cat. Load.	Rate constants (s^{-1})
1	Ph	1%	6.36×10^{-5}
2	2-MeC_6H_4	1%	5.88×10^{-5}
3	4-MeC_6H_4	1%	5.51×10^{-5}
4	2,4,6-$Me_3C_6H_2$	1%	5.77×10^{-5}

5.2 Determination of the reaction order with respect to the catalyst

The reaction order with respect to the catalyst was determined by plotting the concentration of the product against a normalized time scale t[cat]^n (being n the order of the catalyst), according to the method developed by Dr. Burés.[4-5] Visual analysis of the reaction profiles depicted in Figure S16 indicated a first order in **3** (Figure S27c).

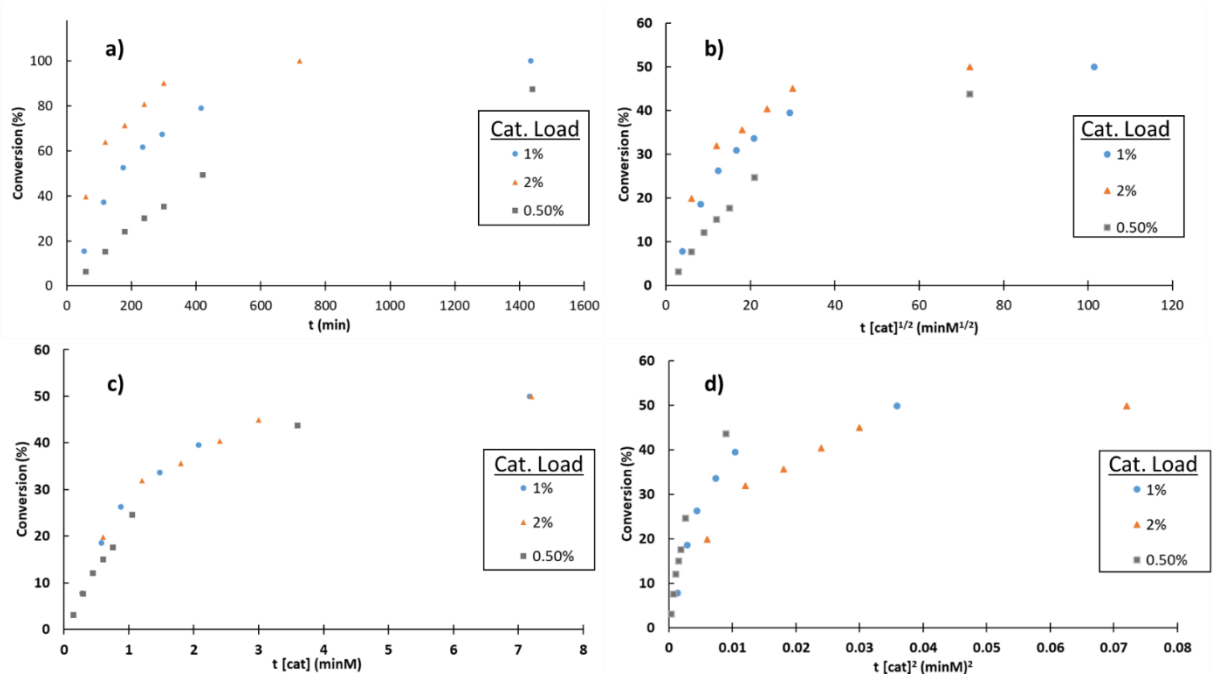

Figure S27. (a) Time-dependent reaction profile of the hydroamination of phenylacetylene with aniline. (b) Reaction profile with normalized time scale assuming a catalyst order of 1/2. (c) Reaction profile with normalized time scale assuming a catalyst order of 1. (d) Reaction profile with normalized time scale assuming a catalyst order of 2.

5.3 Determination of the reaction order with respect to aniline

A stock solution containing catalyst (5 x 0.005 mmol) and NaBAR^F (5 x 0.01 mmol) in 5 mL of CD_3CN was prepared in a Schlenk tube under anaerobic conditions. This solution was then distributed in five (5 x 1 mL) different thick-walled Schlenk tubes fitted with a Teflon cap. Every mixture was stirred at room temperature for 10 min to activate the catalyst. After this time, the appropriate amount of aniline (0.2, 0.5, 0.8, 1.1 and 1.5 mmol) was added to each tube followed by the addition of phenylacetylene (0.5 mmol), and anisole (0.5 mmol) as internal reference. The resulting mixture was stirred at 90°C for the appropriate time. The evolution of the reactions, yields, and conversions were determined by GC analysis comparing the areas of the reagents with the internal standard

and corroborated by ^{1}H NMR spectroscopy. Initial rate plots for different initial concentrations of aniline are given in Figure S28 and the dependence of the initial rate on concentration of aniline is shown in Figure S29.

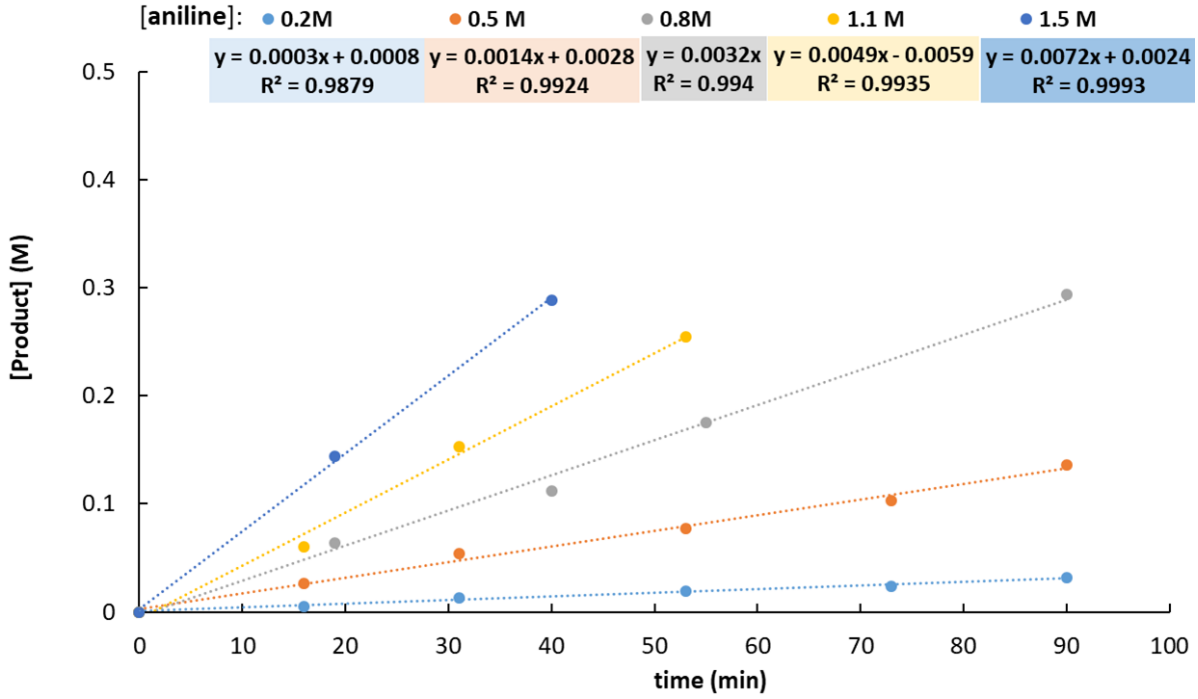

Figure S28. Formation of product over time varying the concentration of aniline.

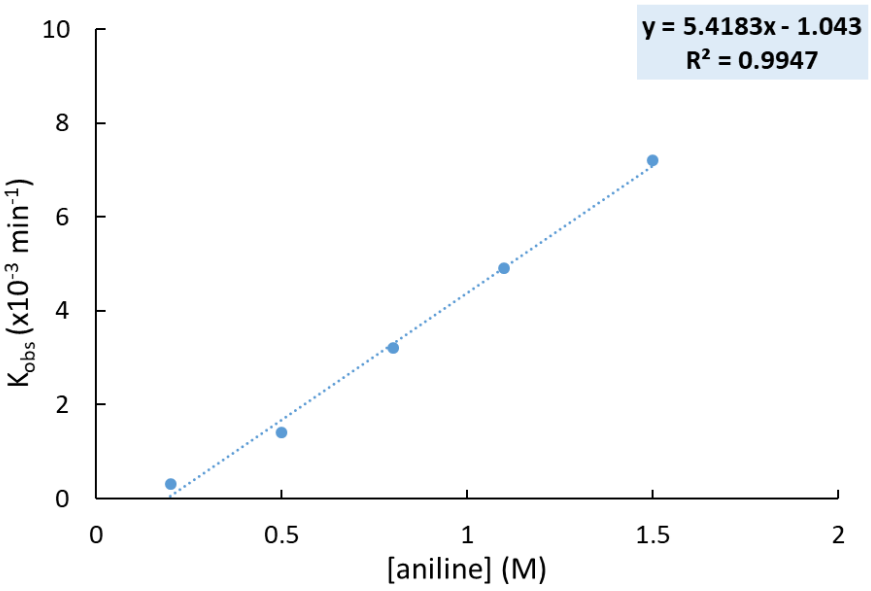

Figure S29. Dependence of the initial rate on the concentration of aniline.

5.4 Determination of the reaction order with respect to phenylacetylene

A stock solution containing catalyst (4 x 0.005 mmol) and $NaBAR^F$ (4 x 0.01 mmol) in 4 mL of CD_3CN was prepared in a Schlenk tube under anaerobic conditions. This solution was then distributed in five (4 x 1 mL) different thick-walled Schlenk tubes fitted with a Teflon cap. Every mixture was stirred at room temperature for 10 min to activate the catalyst. After this time, the appropriate amount of phenylacetylene (0.2, 0.5, 0.8, and 1.1 mmol) was added to each tube followed by the addition of aniline (0.5 mmol) and anisole (0.5 mmol) as internal reference. The resulting mixture was stirred at 90°C for the appropriate time. The evolution of the reactions, yields, and conversions were determined by GC analysis comparing the areas of the reagents with the internal standard and corroborated by ^1H NMR spectroscopy. Initial rate plots for different initial concentrations of phenylacetylene are given in Figure S30 and the dependence of the initial rate on concentration of phenylacetylene is shown in Figure S31.

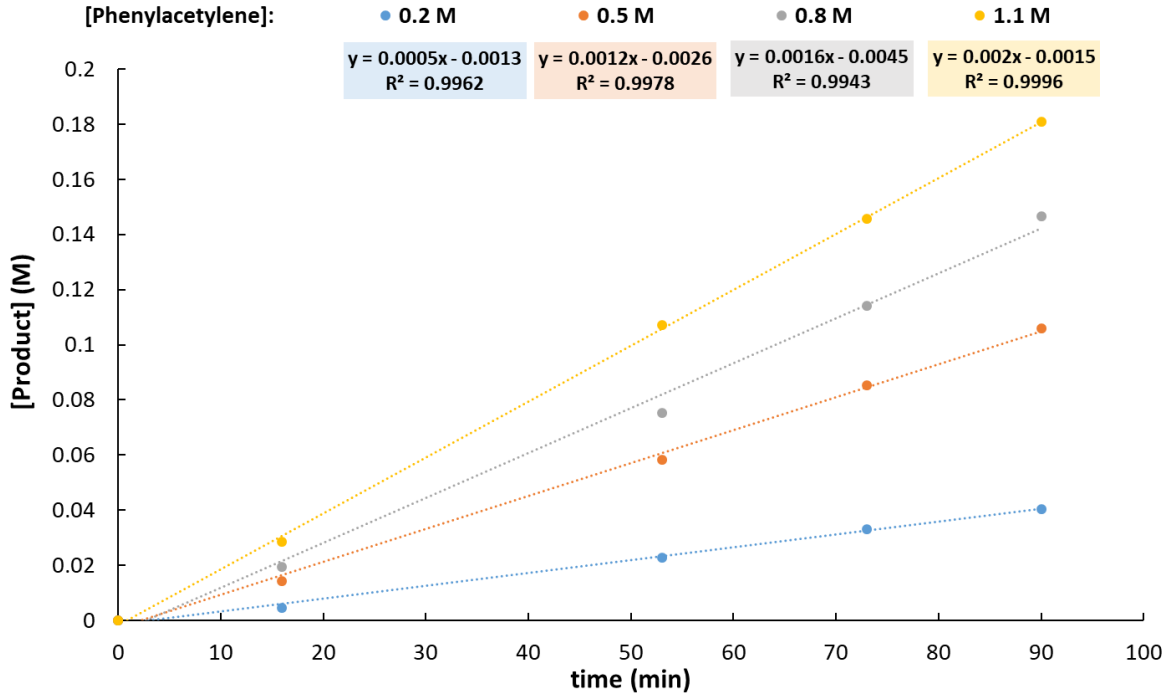

Figure S30. Formation of product over time varying the concentration of phenylacetylene.

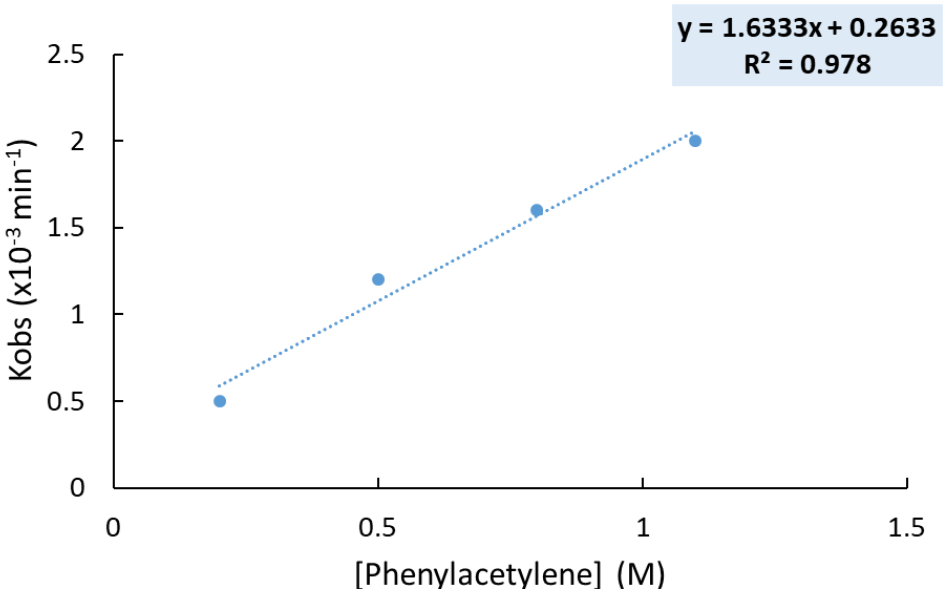

Figure S31. Dependence of the initial rate on the concentration of phenylacetylene.

5.5 Redox switching experiment

A stock solution containing catalyst (2 x 0.005 mmol) and $NaBAR^F$ (2 x 0.01 mmol) in 2 mL of CD_3CN was prepared in a Schlenk tube under anaerobic conditions. This solution was then distributed in two (2 x 1 mL) different thick-walled Schlenk tubes fitted with a Teflon cap. Every mixture was stirred at room temperature for 10 min to activate the catalyst. Subsequently, the corresponding arylamine (2x 0.55 mmol, 1.1 equiv.), phenylacetylene (2 x 0.5 mmol, 1 equiv.), and anisole (2 x 0.5 mmol, 1equiv.) as internal reference were subsequently added under nitrogen. The resulting mixtures were heated at 90 ºC. One reaction was monitored for 7h collecting a small aliquot each 30 min (control reaction). The other one was monitored during 1.5 hours. Afterward, the reductant cobaltocene was added to the mixture (1.5 equivalent with respect to catalyst). The addition of cobaltocene produced a complete deactivation of the catalytic activity. After collecting data for the following 1 hours, 1.5 equivalent (with respect to catalyst) of a chemical oxidant, namely $[Fe(\eta_5\text{-}C_5H_4COCH_3)Cp][BF_4]$, was added to the reaction mixture under nitrogen. The activity of the catalyst was completely restored by addition of the oxidant. The oxidant and the reductant were sequentially added separated by periods of different times and the evolution of the reaction was monitored by GC.

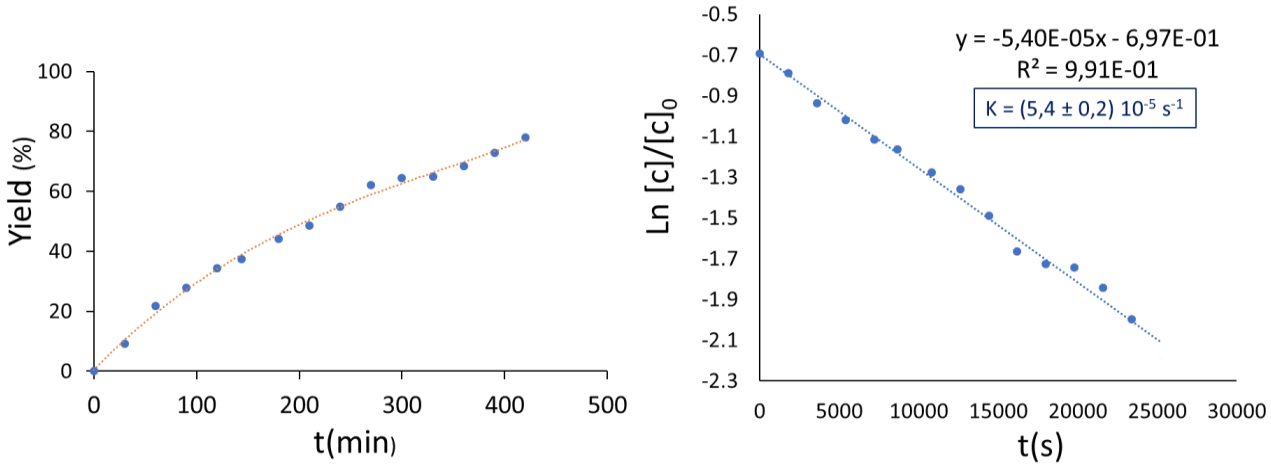

Figure S32. Plot showing the hydroamination of phenylacetylene of the control reaction and non-linear least squares fit of the kinetic data.

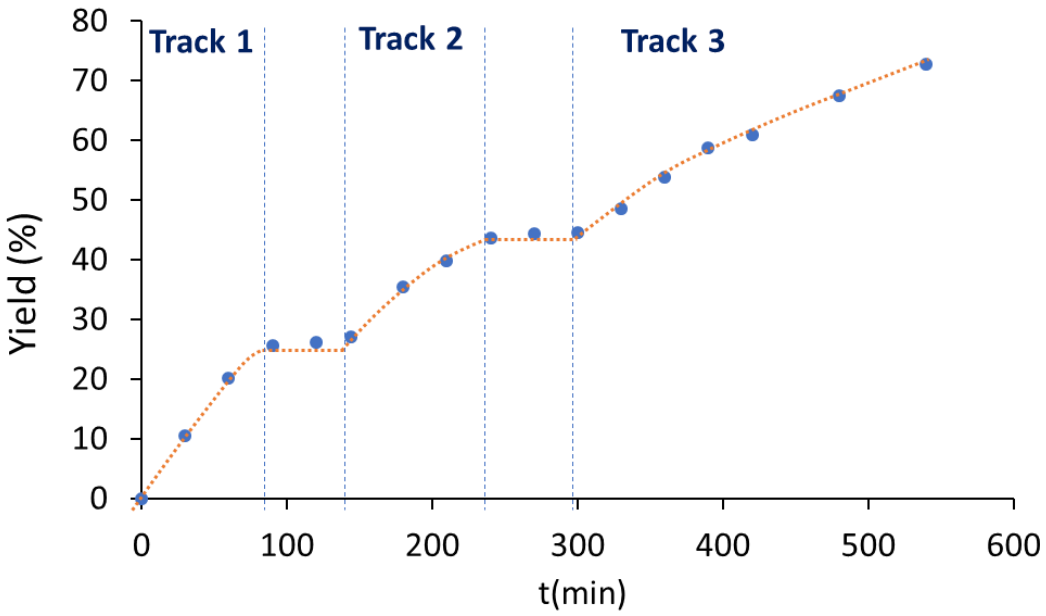

Figure S33. Switching experiment of the hydroamination of phenylacetylene with aniline with sequential additions of [Cp_2Co] and [Fe(η_5-$C_5H_4COCH_3$)Cp][BF_4].

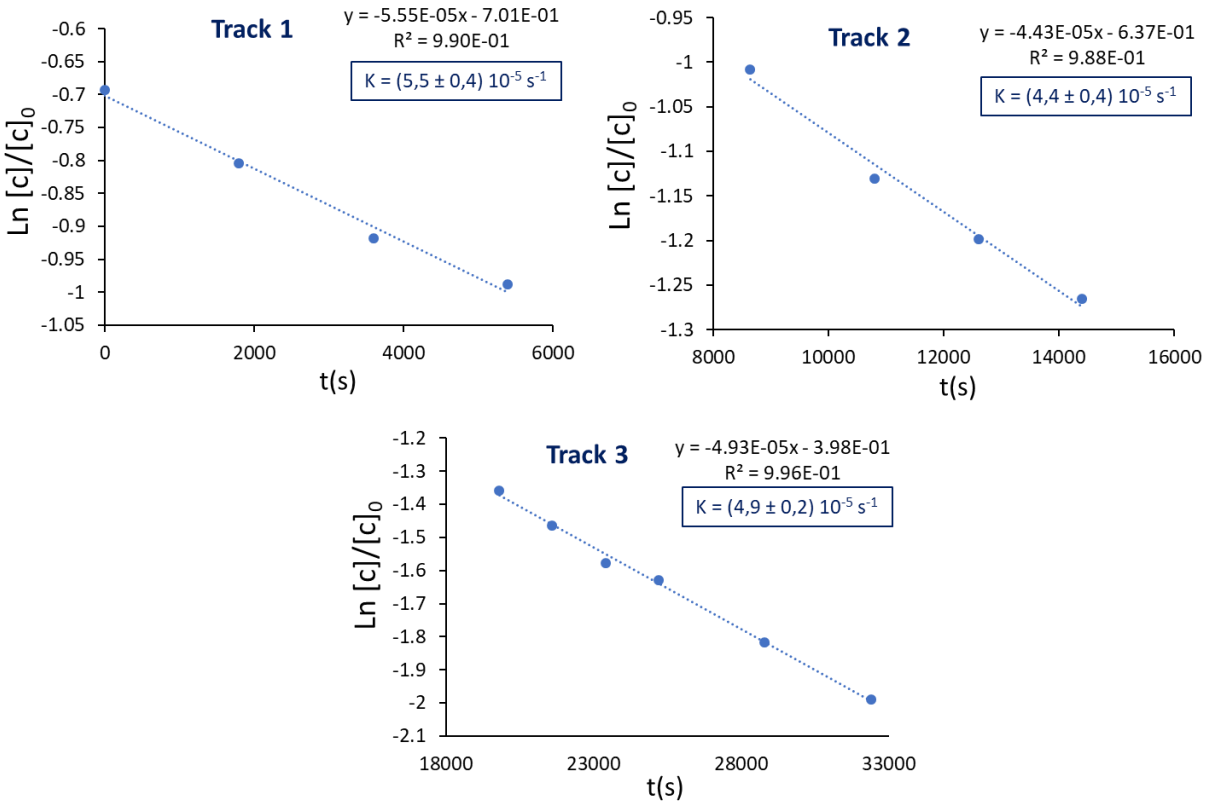

Figure S34. Non-linear least squares fit of the different tracks of the switching experiment.

6. References

1. Ruiz-Zambrana, C.; Gutierrez-Blanco, A.; Gonell, S.; Poyatos, M.; Peris, E., Redox-Switchable Cycloisomerization of Alkynoic Acids with Napthalenediimide-Derived N-Heterocyclic Carbene Complexes. *Angew. Chem., Int. Ed.* **2021,** *60*, 20003-20011.

2. Wang, H. L.; Chen, L. C.; Xiao, Y., Heterologous perylene diimide arrays: potential non-fullerene acceptors in organic solar cells. *J. Mater. Chem. C* **2017,** *5*, 8875-8882.

3. Gonell, S.; Poyatos, M.; Peris, E., Triphenylene-Based Tris(N-Heterocyclic Carbene) Ligand: Unexpected Catalytic Benefits. *Angew. Chem., Int. Ed.* **2013,** *52*, 7009-7013.

4. Bures, J., Variable Time Normalization Analysis: General Graphical Elucidation of Reaction Orders from Concentration Profiles. *Angew. Chem., Int. Ed.* **2016,** *55*, 16084-16087.

5. Bures, J., A Simple Graphical Method to Determine the Order in Catalyst. *Angew. Chem., Int. Ed.* **2016,** *55*, 2028-2031.